

# DELIVERABLE 3.1

---

## Climate change assessment: Observational based study

---

***Let's be reSEAlient!***



## Project key facts

<b>Priority:</b>	2. Safety and resilience
<b>Specific objective:</b>	2.1 Improve the climate change monitoring and planning of adaptation measures tackling specific effects in the cooperation area
<b>Acronym:</b>	<b>RESPONSe</b>
<b>Title:</b>	<b>Strategies to adapt to climate change in Adriatic regions</b>
<b>ID request:</b>	10175714
<b>Lead Partner:</b>	INFORMEST
<b>Duration:</b>	01.01.2019      30.06.2021

## Deliverable information

<b>WP 3</b>	Harmonization of the climate change analysis and monitoring systems
<b>A 1</b>	Analysis of observed data
<b>Issued by:</b>	<b>Partner n°6 – DHMZ</b>
<b>Reviewed by:</b>	<b>All project partners</b>
<b>Partners involved:</b>	<b>Apulia region, Institute of oceanography and fisheries, Croatian meteorological and hydrological service, Regional agency for environmental protection and prevention of Veneto, University polytechnic of Marche</b>
<b>Status:</b>	Final
<b>Distribution:</b>	Public
<b>Date:</b>	31.3.2020

## Document history

Version	Date	Author	Description of changes
V 0.1	15.10.2019.	DHMZ	Table of content defined, and first contributions included
Final	31.03.2020	DHMZ	Numbers check and minor revision done.

## Table of contents

<b>Introduction and methodology .....</b>	<b>3</b>
<b>Results and discussion .....</b>	<b>5</b>
1 Temperature and precipitation: mean climate over Adriatic region.....	5
2 Temperature and precipitation: linear trends over the Adriatic region.....	10
3 Temperature and precipitation: annual time-series over the selected locations .....	15
4 Examples of user targeted climate analysis.....	30
Climate Index for Tourism.....	30
Heating and Cooling Degree Days.....	37
Extreme precipitation return periods .....	41
Wind speed and wind gusts trends.....	45
5 Sea temperature trends in the Adriatic .....	51
Introduction .....	51
Data and method .....	51
Trend analyses .....	53
Results.....	53
Conclusion and discussion .....	58
6 Sea level trends in the Adriatic .....	59
7 Sea temperature and salinity trends in the Adriatic transect.....	63
<b>Acknowledgements .....</b>	<b>64</b>
<b>References .....</b>	<b>65</b>
<b>Appendix: Station observations of the meteorological parameters .....</b>	<b>67</b>
<b>Table A1 Basic meta-data of the analysed meteorological observations. ....</b>	<b>67</b>

## Introduction and methodology

The purpose of this deliverable is to provide harmonized analysis of historical climate over the Adriatic region, more specifically, over the location of the RESPONSE pilot areas. Description of the Activity 1 based on the RESPONSE Application form provides following setups:

*“Climatological data from the DHMZ and ARPAV WS meteorological networks in coastal area will be employed for detection of climate change from 1961 to 2016. At the locations where specific observations exist for the common period, the trends in mean air temperature, precipitation amounts and wind gust as well as in the corresponding indices of extremes will be performed. Additionally, annual maxima of short-term precipitation amounts will be analysed by means of the extreme value theory. Oceanographic variables’ trends (sea level, temperature and salinity) will be assessed on monthly mean reanalyses data from 1961 to 2016 over the Adriatic basin. Sea temperature, salinity and sea level data from the IOF database MEDAS and long-term operating tide gauges will be used for detection of climate change and regimes in the same period over the eastern Adriatic”.*

In addition, Activity 1 deliverables is envisioned to include following elements in the analysis:

*“This deliverable will provide climate change and climate regime assessments based on existing meteorological, climate and oceanographic data over the Adriatic sea and the Adriatic coast. Focus will be given to the project case study areas (Veneto coastal area, Island of Cres, River Krka estuary, Dubrovačko-Neretvanska County), and the general overview over the entire Adriatic region will be given. It will provide an improved knowledge of sea flooding in the coastal area, and on the statistics of the extreme weather and climate events in the recent observational period. The results of this deliverable will be basis for the evaluation of the regional climate models for the historical period in Act. 3.2. The climate potential of tourism will be analysed by means of climate index for tourism (CIT) for present and future climate. CIT integrates thermal, aesthetic and physical facets of atmospheric environment important for different types of tourism activities. Also, energy demands for cooling and heating will be considered using specific climatological indicators.”*

Taking into account planned research activities, the results presented in this deliverable include:

1. The analysis of the E-OBS 19.0 gridded dataset for the mean annual and seasonal temperature (mean, maximum, minimum) and total precipitation amount and corresponding linear trends.
2. For the location of the selected cities along the Croatian and Italian coast, the time-series of the mean annual maximum and minimum temperature and annual number of summer days (days when maximum daily temperature  $> 25$  °C) and annual number of tropical nights (days when minimum daily temperature  $> 20$  °C) based on the local observations (where available) and extracted and estimated from the E-OBS 19.0 dataset.
3. Similarly as for the previous point but for the annual number of wet days (days when total daily precipitation  $RR \geq 1$  mm), annual number of heavy precipitation days (days when total daily precipitation  $RR \geq 20$  mm), annual number of consecutive dry days (CDD) periods (period of at least 5 days with total daily precipitation  $RR \leq 1$  mm) and annual number of consecutive wet days (CWD) periods (period of at least 5 days with total daily precipitation  $RR \geq 1$  mm) and mean annual precipitation amount.

4. The analysis of the extreme precipitation amounts for the selected return periods (based on the E-OBS 19.0 dataset (Cornes et al., 2018)), heating and cooling degree days (also based on the E-OBS 19.0 dataset), Climate Index for Tourism (CIT; based on the ERA5 reanalysis (C3S, 2017)) and 10-m wind speed (based on the ERA5 reanalysis) for the locations from the focus areas of the RESPONSe project (Italy: Lignano Sabiadoro, Montermarciano and Brindisi; Croatia: Cres, Šibenik, Dubrovnik).
5. Analysis of the ocean data available over the region, including several locations with the high-quality long term observations of the sea surface temperature, sea level height and sea temperature & salinity through the Adriatic transect and available through the IZOR MEDAS database.

Results presented in this deliverables should be considered indicative and as a demonstration of possible harmonized analysis of the atmospheric and oceanographic variables over the Adriatic region. For the specific locations more specific analysis may be performed using the same data source. Also, the approach was to use latest versions of the most relevant datasets in the climate community (E-OBS 19.0 gridded dataset and ECMWF/Copernicus ERA5 reanalysis) when no local observations were present or were present in a limited frequency or time span. It is also important to stress the limitations of the E-OBS and similar products. Their quality depends on the underlying station density used in the product preparation, and the limits in the interpolation algorithms. The values from the E-OBS dataset also represent mean values over its grid (approximately, 12.5 km x 12.5 km in the E-OBS 19.0), which leads to e.g. precipitation underestimation in E-OBS when compared to actual extreme precipitation events observed at the local stations (when available).

Finally, the performed analysis was done in a harmonized approach for all locations considered, and provides joint overview of the status of the several relevant meteorological and oceanographic quantities along the Adriatic. This deliverable coming from the Activity 1 in the WP3 will be basis for the next steps in the same working package of the RESPONSe project.

## Results and discussion

### 1 Temperature and precipitation: mean climate over Adriatic region

This subsection provides spatial maps of mean annual temperatures and precipitation amount (Fig. 1.1), and seasonal means of the same quantities (Fig. 1.2. to 1.5.). It summarizes the main climate characteristics over the broader Adriatic region estimated from the E-OBS (version 19.0; Cornes et al. 2018) gridded dataset.

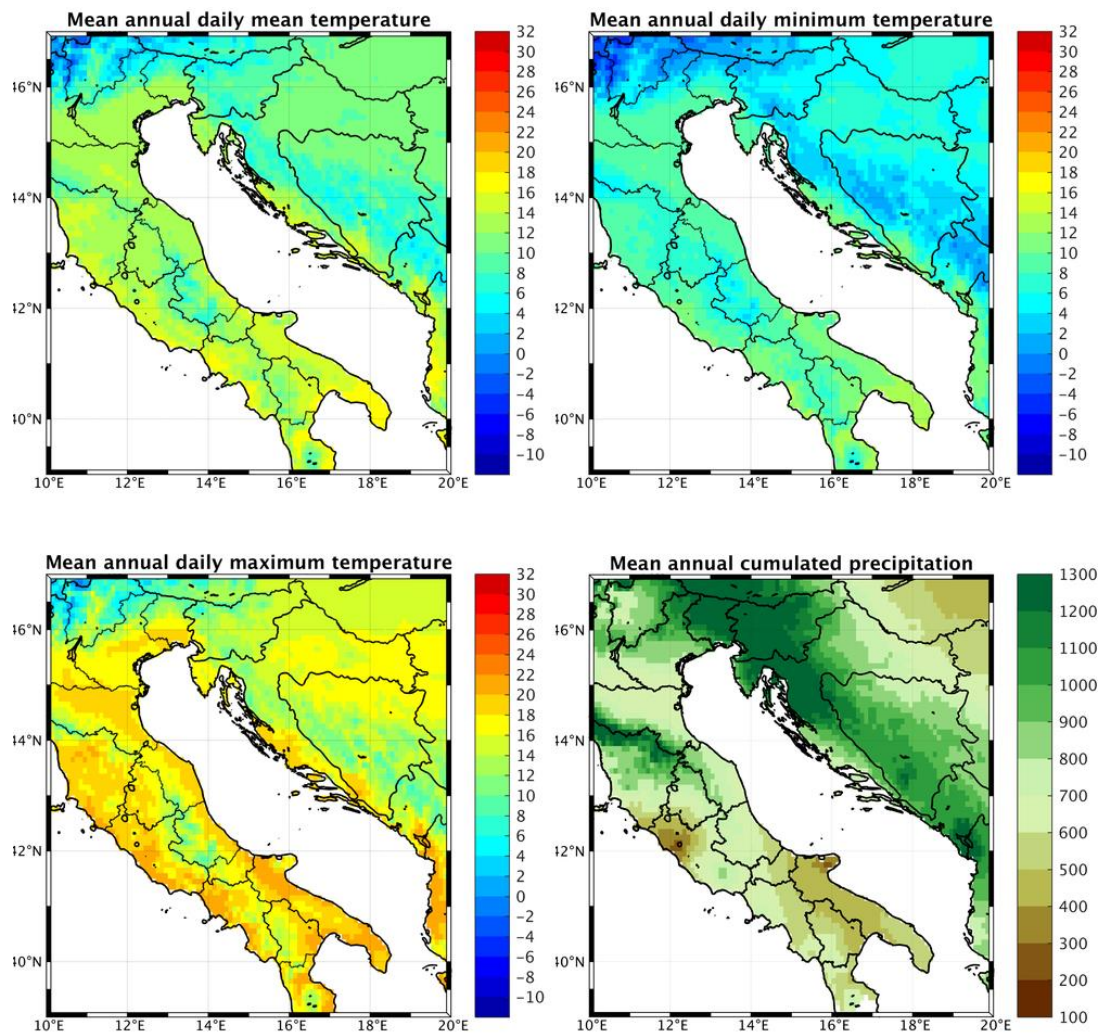


**Figure 1.1:** Mean annual daily mean temperature (TG; units: °C), daily minimum temperature (TX; units: °C), daily maximum temperature (TX; units: °C) and mean annual total precipitation amount (RR; units: mm). Data source: E-OBS, data period: 1961-2018.

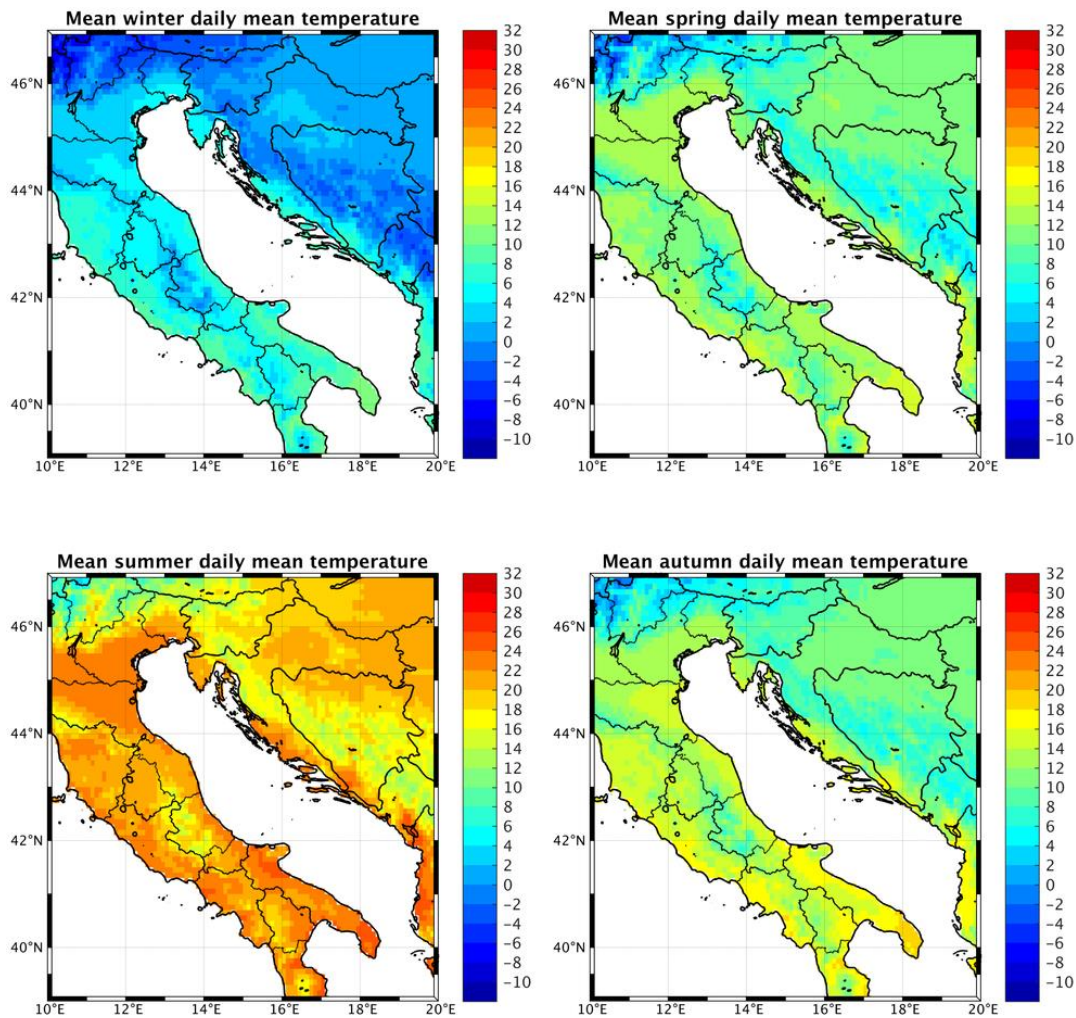


**Figure 1.2:** Mean seasonal daily mean temperature (TG; units: °C). First row winter (DJF) and spring (MAM); second row: summer (JJA) and autumn (SON). Data source: E-OBS, data period: 1961-2018.

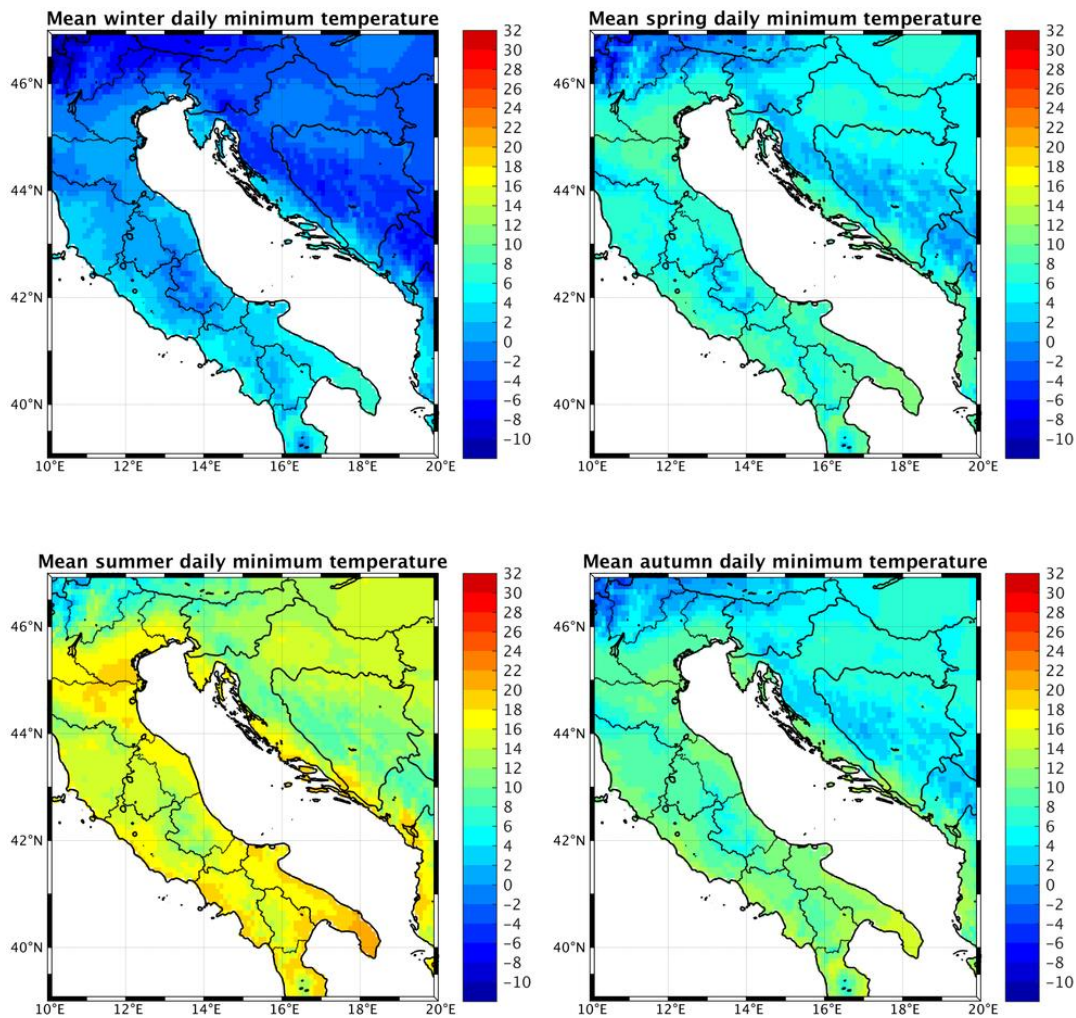


**Figure 1.3:** Mean seasonal daily minimum temperature (TN; units: °C). First row winter (DJF) and spring (MAM); second row: summer (JJA) and autumn (SON). Data source: E-OBS, data period: 1961-2018.

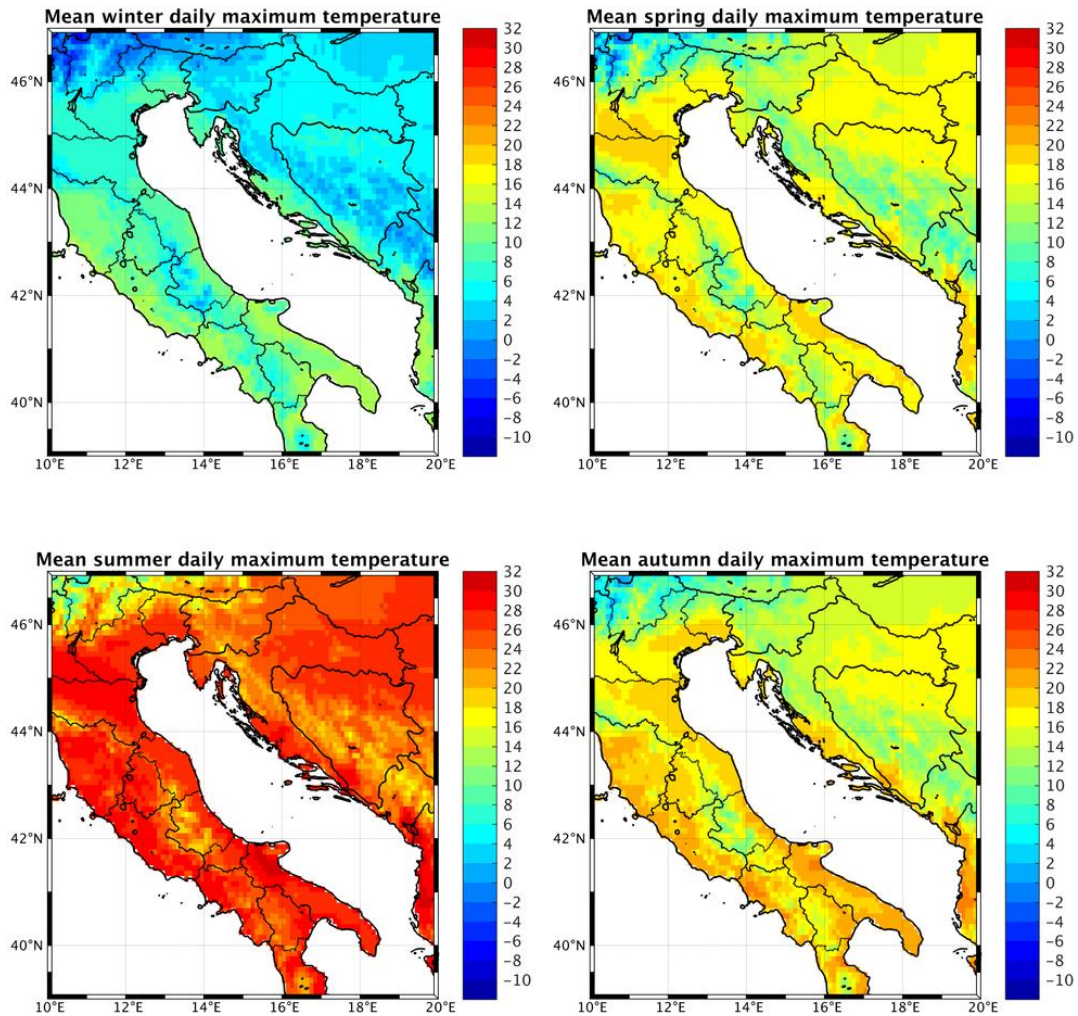


**Figure 1.4:** Mean seasonal daily maximum temperature (TX; units: °C). First row winter (DJF) and spring (MAM); second row: summer (JJA) and autumn (SON). Data source: E-OBS, data period: 1961-2018.

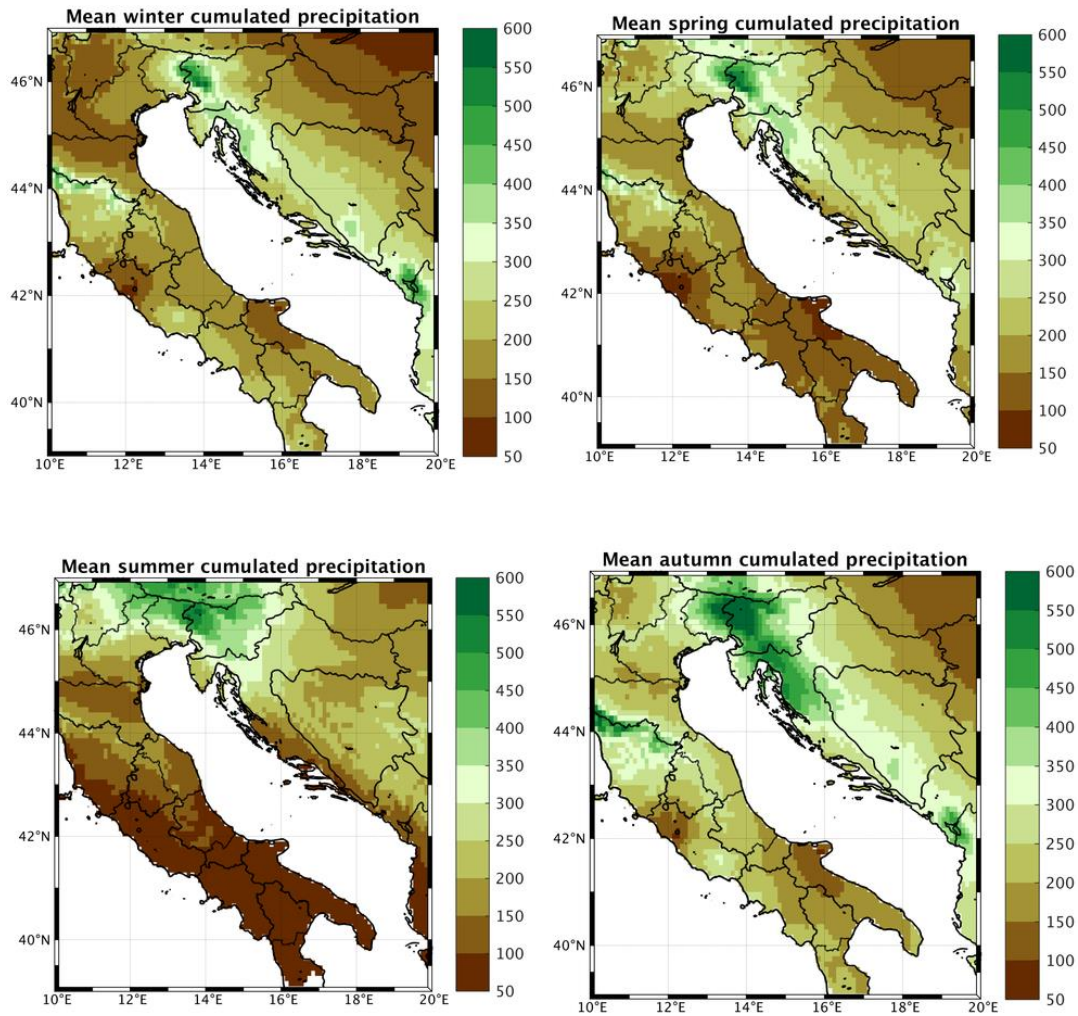


**Figure 1.5:** Mean seasonal total precipitation amounts (RR; units: mm). First row winter (DJF) and spring (MAM); second row: summer (JJA) and autumn (SON). Data source: E-OBS, data period: 1961-2018.

## 2 Temperature and precipitation: linear trends over the Adriatic region

This subsection provides spatial maps of linear trends of the mean annual and seasonal temperatures and precipitation amount (Fig. 2.1 to 2.4) based on the E-OBS v19.0 dataset (Cornes et al., 2018), for the period 1961 – 2018. While temperature trends based on the annual and seasonal means of daily mean, minimum and maximum temperatures are positive and statistically significant over most of the region and in all seasons, the linear trends in terms of the precipitation amounts show large variability in terms of the sign (both positive and negative trends are documented), amplitude and are rarely statistically significant.

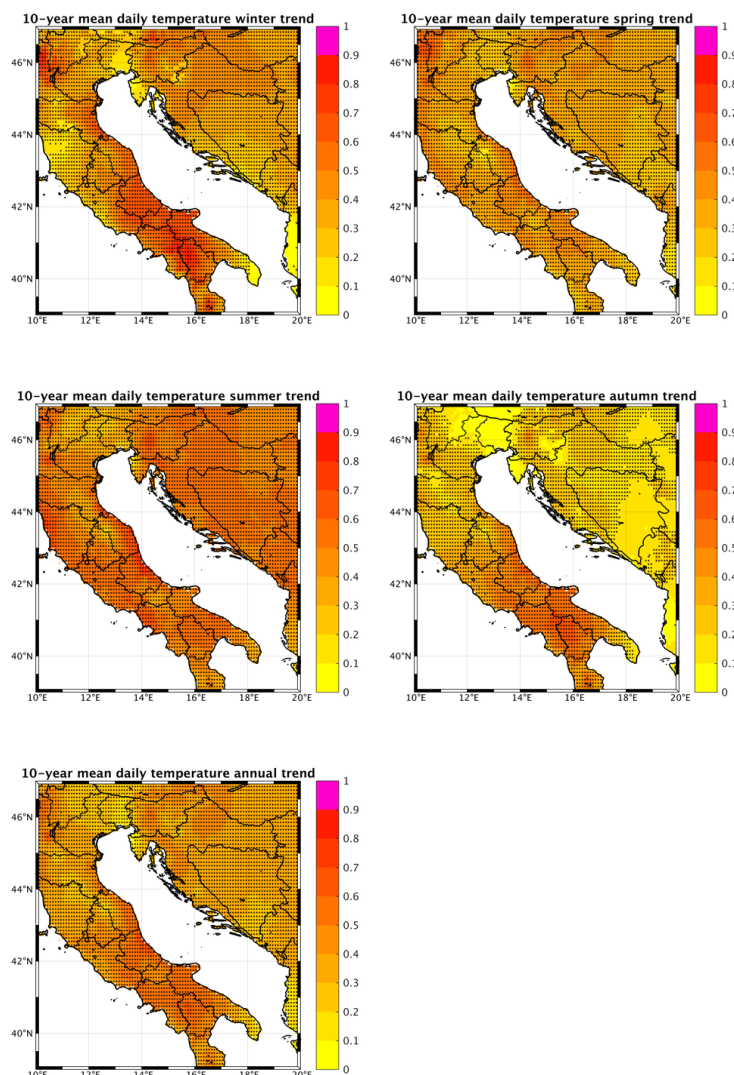


**Figure 2.1:** Linear trends in the mean seasonal and annual daily mean temperature (TG; units: °C/10 years). First row: First row: winter (DJF) and spring (MAM); second row: summer (JJA) and autumn (SON); third row: year. Dotted: statistically significant trends according to the Mann-Kendall significance test at the  $\alpha=0.05$ . Data source: E-OBS, data period: 1961-2018.

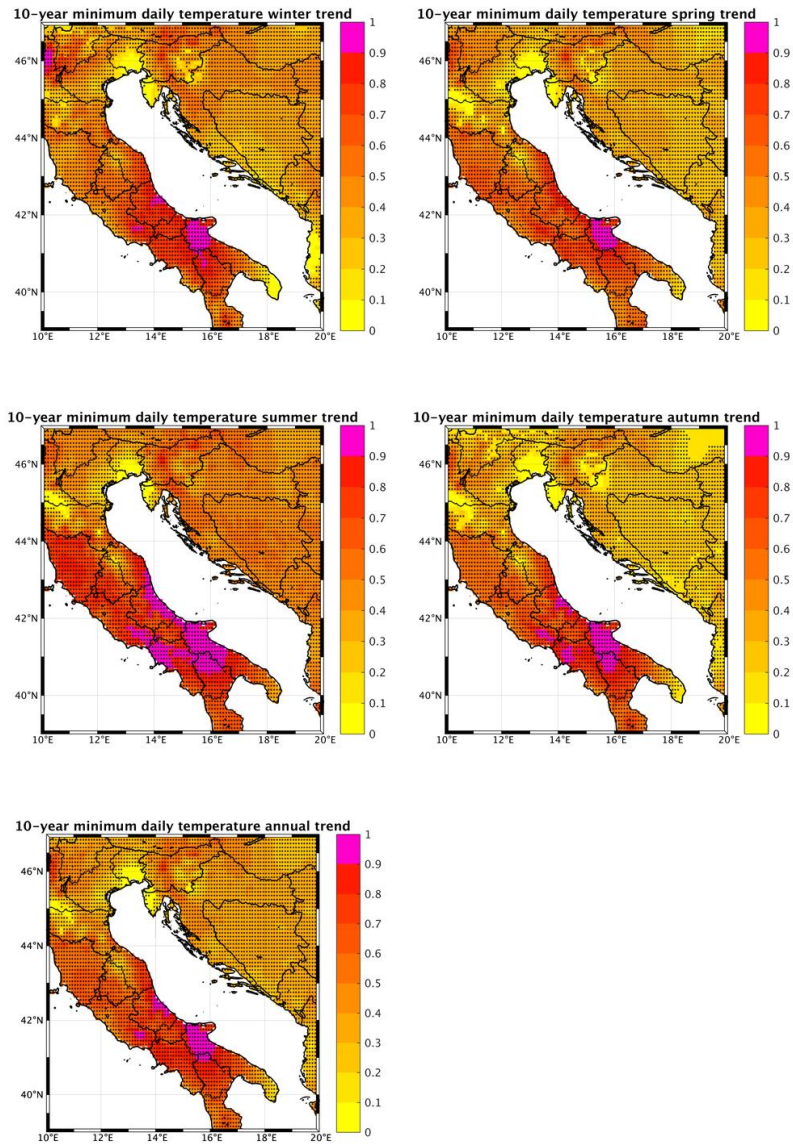


**Figure 2.2:** Linear trends in the mean seasonal and annual daily minimum temperature (TN; units: °C/10 years). First row: First row: winter (DJF) and spring (MAM); second row: summer (JJA) and autumn (SON); third row: year. Dotted: statistically significant trends according to the Mann-Kendall significance test at the  $\alpha=0.05$ . Data source: E-OBS, data period: 1961-2018.

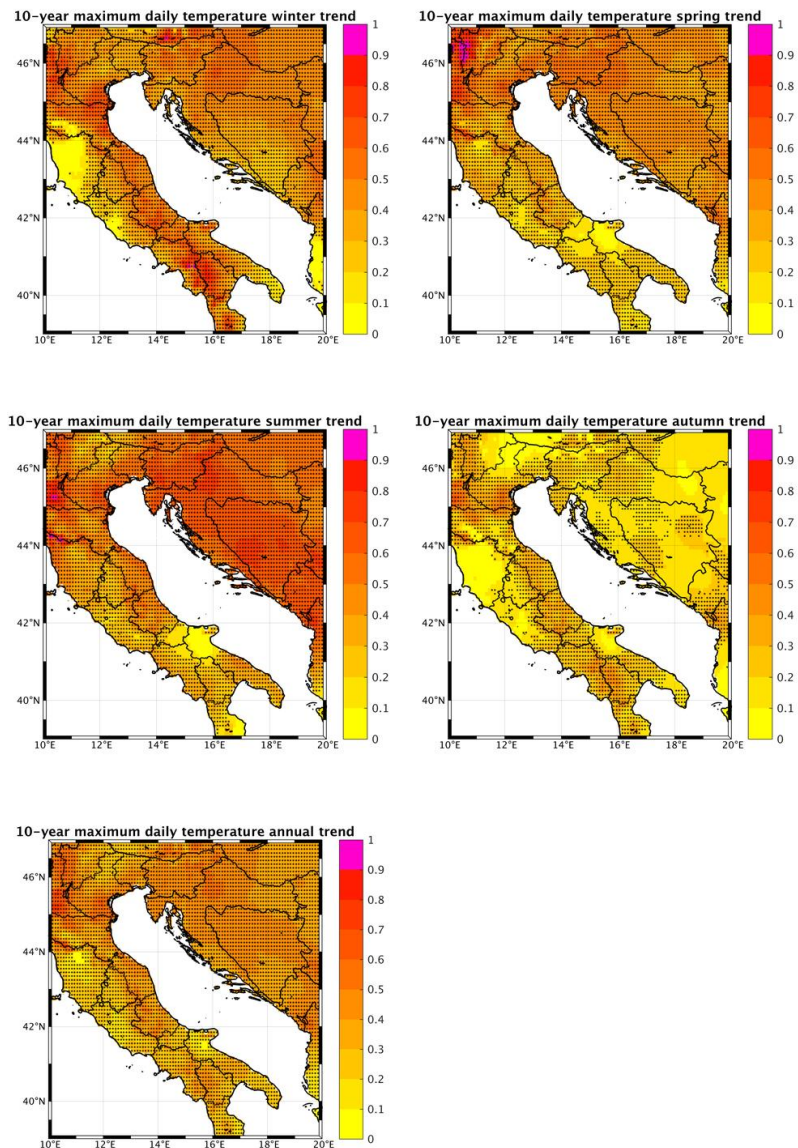


**Figure 2.3:** Linear trends in the mean seasonal and annual daily maximum temperature (TX; units: °C/10 years). First row: First row: winter (DJF) and spring (MAM); second row: summer (JJA) and autumn (SON); third row: year. Dotted: statistically significant trends according to the Mann-Kendall significance test at the  $\alpha=0.05$ . Data source: E-OBS, data period: 1961-2018.

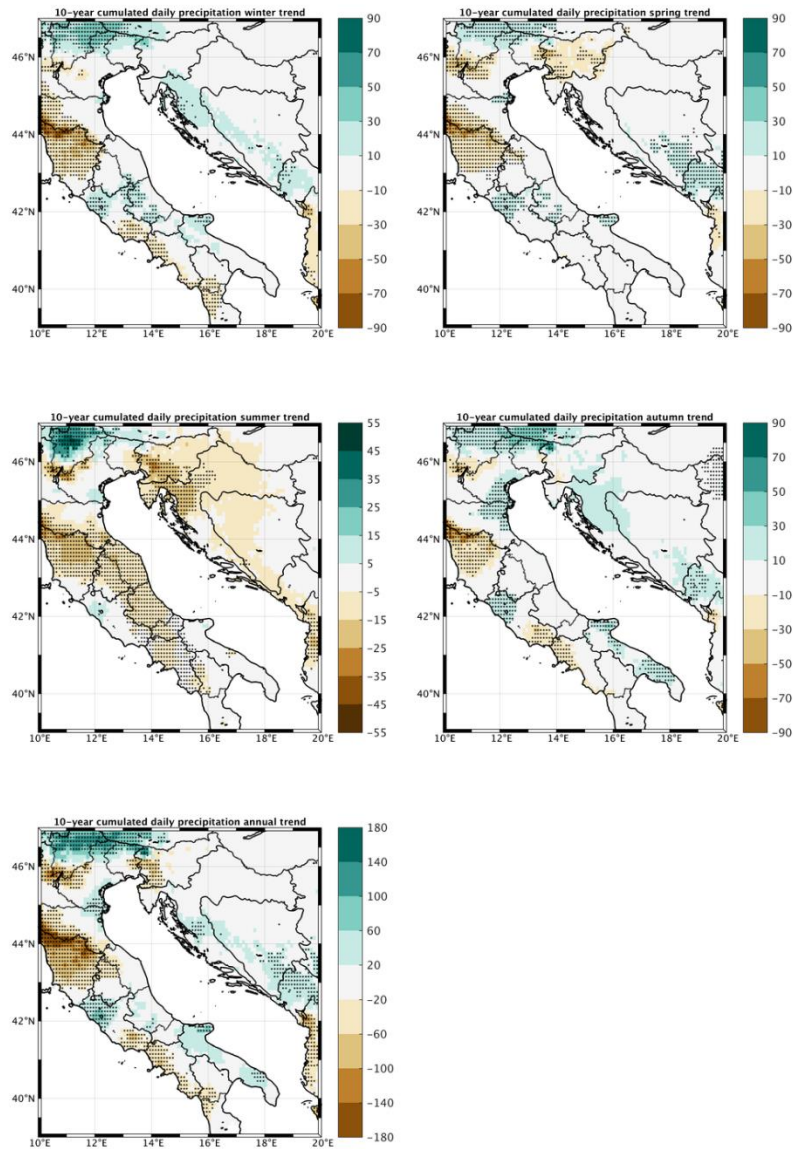


**Figure 2.4:** Linear trends in the mean seasonal and annual total precipitation amounts (RR; units: mm/10 years). First row: First row: winter (DJF) and spring (MAM); second row: summer (JJA) and autumn (SON); third row: year. Dotted: statistically significant trends according to the Mann-Kendall significance test at the  $\alpha = 0.05$ . Data source: E-OBS, data period: 1961-2018.

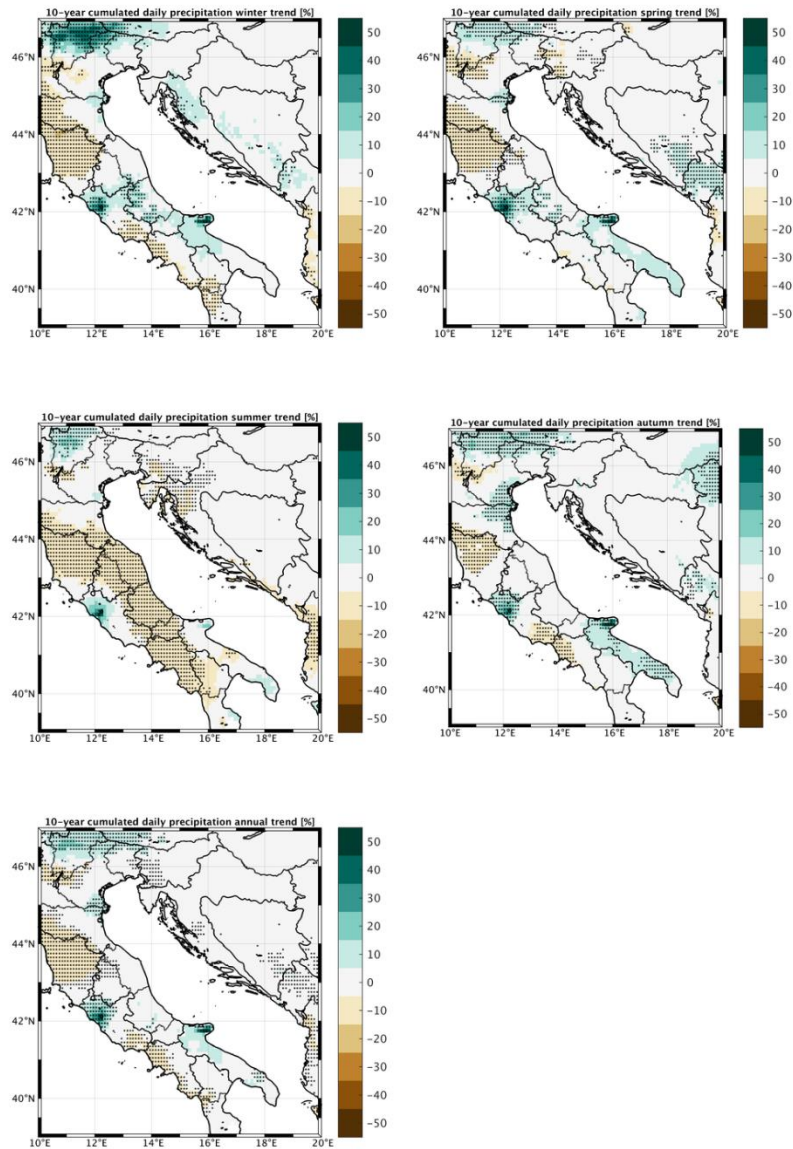


**Figure 2.5:** Linear trends (relative with respect to the mean values during the 1961-1990 period) in the mean seasonal and annual total precipitation amounts (RR; units: %/10 years). First row: First row: winter (DJF) and spring (MAM); second row: summer (JJA) and autumn (SON); third row: year. Dotted: statistically significant trends according to the Mann-Kendall significance test at the  $\alpha = 0.05$ . Data source: E-OBS, data period: 1961-2018.

### 3 Temperature and precipitation: annual time-series over the selected locations

In this subsection, time-series of several relevant climate variables and indices are presented and summarized. Two types of climate information are considered: (1) local observations and (2) estimates based for the same locations extracted from the E-OBS v19.0 dataset (Cornes et al., 2018). Although local observations are considered as the primary source of the climate information, due to the gaps in the time-series, we estimate the share of the missing year (here rather strict approach is performed: if there is any missing value for specific year, the whole years is removed from the subsequent graphical presentation and marked as missing data), the Pearson correlation coefficient between two time-series for each location and the estimation the linear trends based on the E-OBS time-series (also with the provision of the information related to the statistical significance).

Results are presented for

- (1) Three Croatian stations in Figs 3.1 and 3.2.
- (2) Four stations from the Friuli-Venezia-Giulia region in Figs. 3.3 and 3.4.
- (3) Six stations from the Veneto region in Figs. 3.5 and 3.6.
- (4) Five stations from the Emilia-Romagna region in Figs. 3.7 and 3.8.
- (5) Three stations from the Marche region in Figs. 3.9 and 3.10.
- (6) Four stations from the Abruzzo region in Figs. 3.11 and 3.12.
- (7) Five stations from the Puglia region in Figs. 3.13 and 3.14.

In summary, majority of the temperature related variables and indices shows rising and statistically significant changes, while changes in precipitation related variables and indices are more local specific. In some cases the time-series based on local observations and E-OBS v19.0 are shifted one from another, but even in these cases linear correlation coefficient is positive and high.

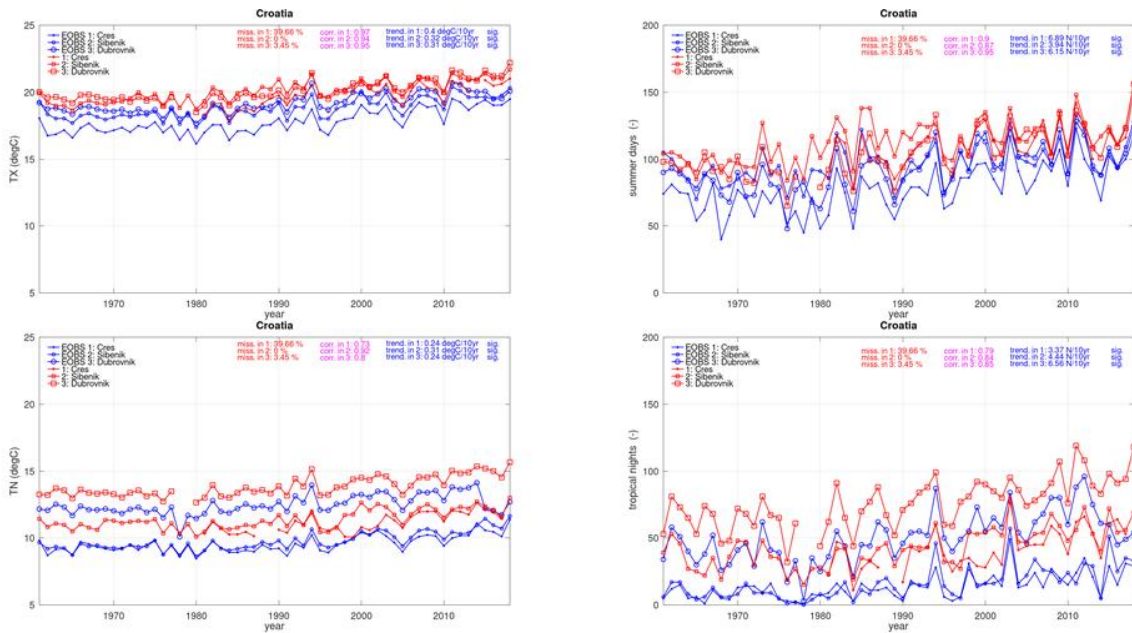


**Figure 3.1** First column: time-series of the mean annual daily maximum temperature (TX; units: °C) and mean annual daily minimum temperature (TN; units: °C). Second column: annual number of summer days (days when TX>25 °C) and annual number of tropical nights (days when TN>20 °C). Stations: selected three locations along the Croatian coast. Time period considered: 1961-2018. Data source: E-OBS (in blue) and local station data (in red). Additional information: the share of the missing years (for simplicity the missing year is defined if at least one daily observation is missing) in the local data (in red), the linear correlation coefficient between E-OBS and local station data (in magenta), linear trend from the E-OBS based time-series (with the results of the Mann Kendall significance test at the  $\alpha = 0.05$ ; in blue). Separate graphs for each location are available in Supplemental material to this deliverable.

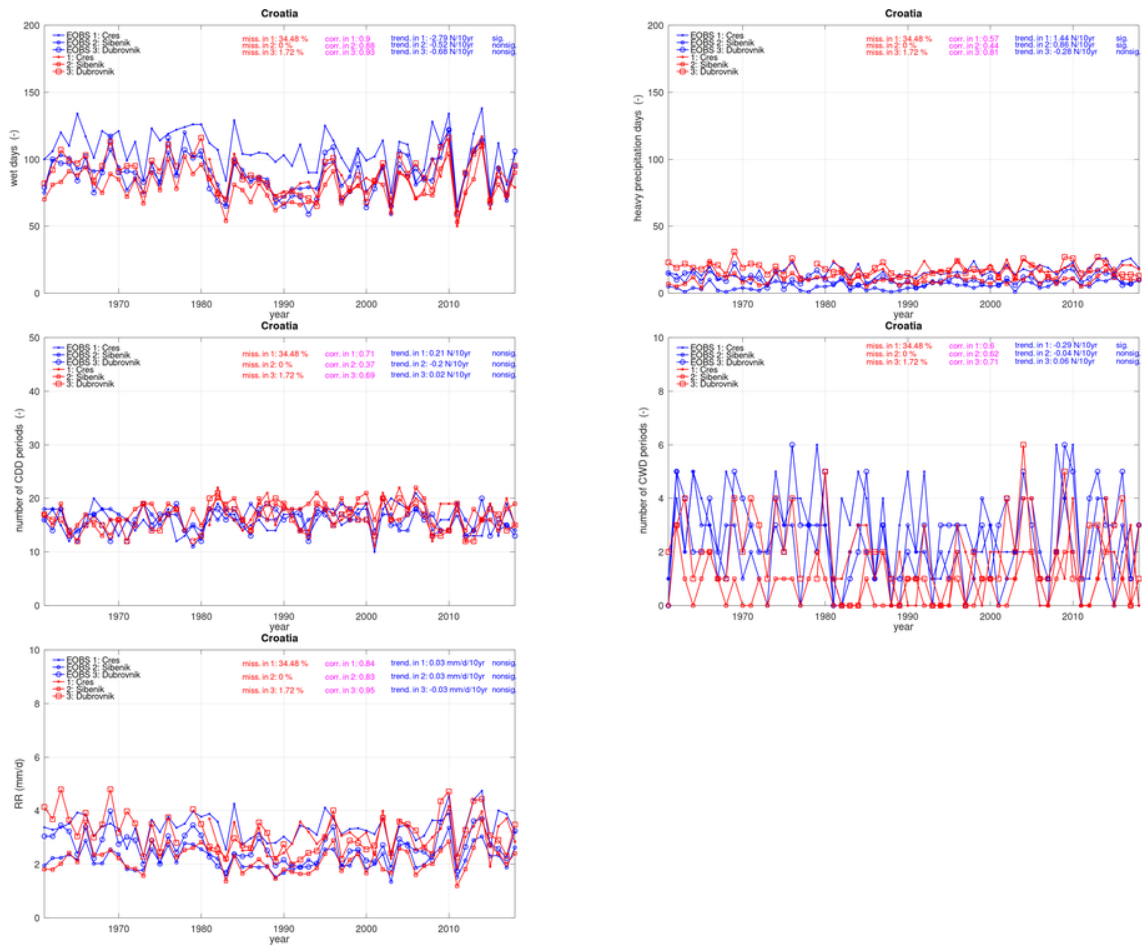


**Figure 3.2** First row: time-series of the annual number of wet days (days when total daily precipitation  $RR \geq 1$  mm) and annual number of heavy precipitation days (days when total daily precipitation  $RR \geq 20$  mm). Second row: annual number of consecutive dry days (CDD) periods (period of at least 5 days with total daily precipitation  $RR \leq 1$  mm) and annual number of consecutive wet days (CWD) periods (period of at least 5 days with total daily precipitation  $RR \geq 1$  mm). Third row: time-series of the total annual precipitation amounts (RR; units: mm/day). Stations: selected three locations along the Croatian coast. Time period considered: 1961-2018. Data source: E-OBS (in blue) and local station data (in red). Additional information: the share of the missing years (for simplicity the missing year is defined if at least one daily observation is missing) in the local data (in red), the linear correlation coefficient between E-OBS and local station data (in magenta), linear trend from the E-OBS based time-series (with the results of the Mann Kendall significance test at the  $\alpha = 0.05$ ; in blue). Separate graphs for each location are available in Supplemental material to this deliverable.

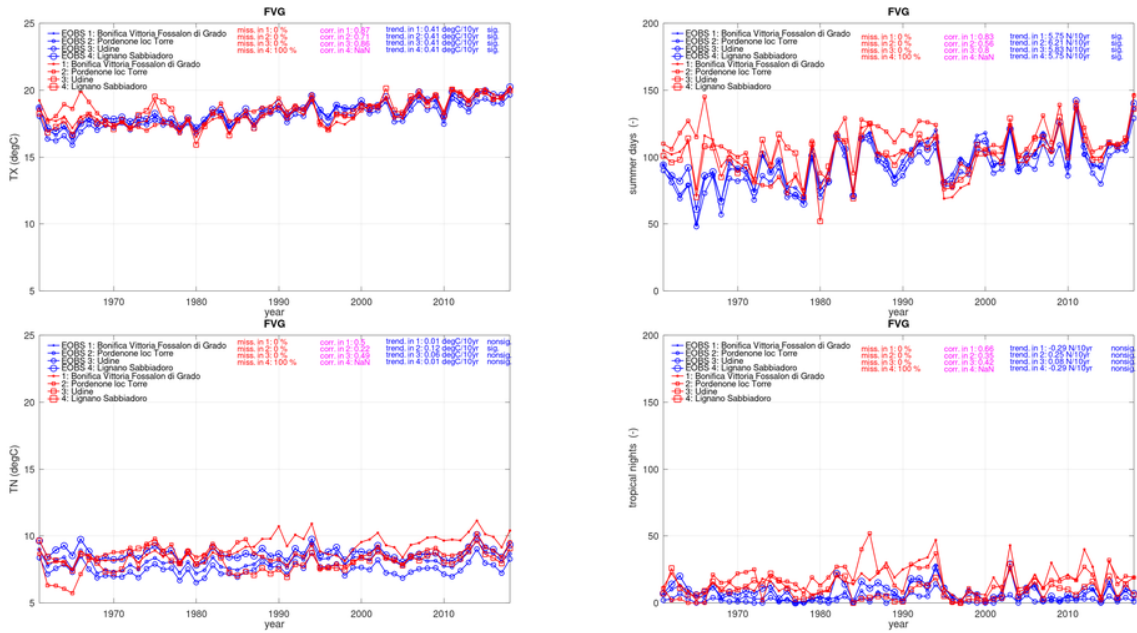


**Figure 3.3** Same as Fig. 3.1 but for the selected three locations from the Italian region Friuli-Venezia-Giulia. Separate graphs for each location are available in Supplemental material to this deliverable.



**Figure 3.4** Same as Fig. 3.2 but for the selected three locations from the Italian region Friuli-Venezia-Giulia. Separate graphs for each location are available in Supplemental material to this deliverable.

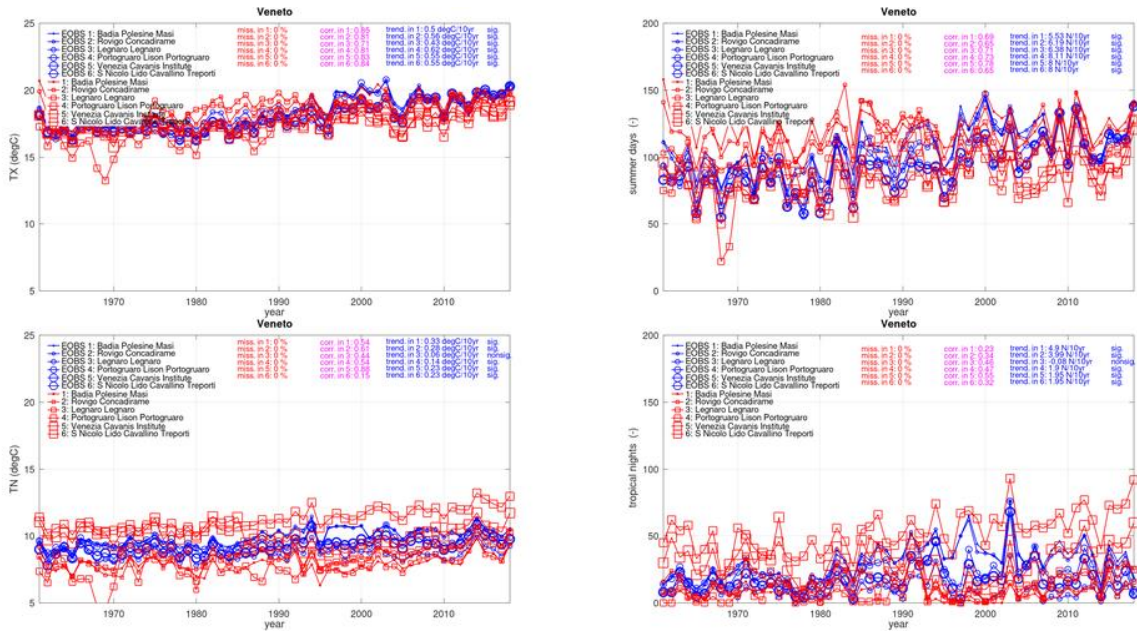
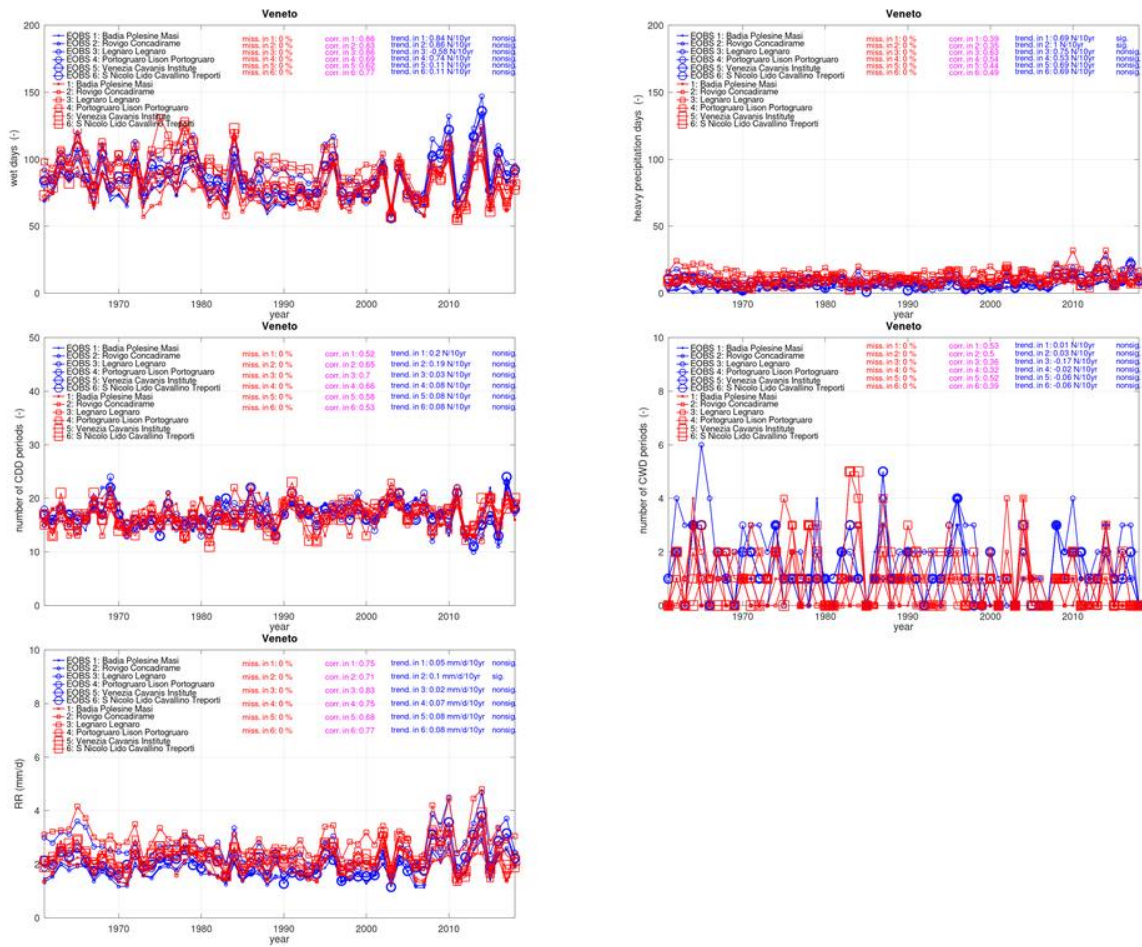
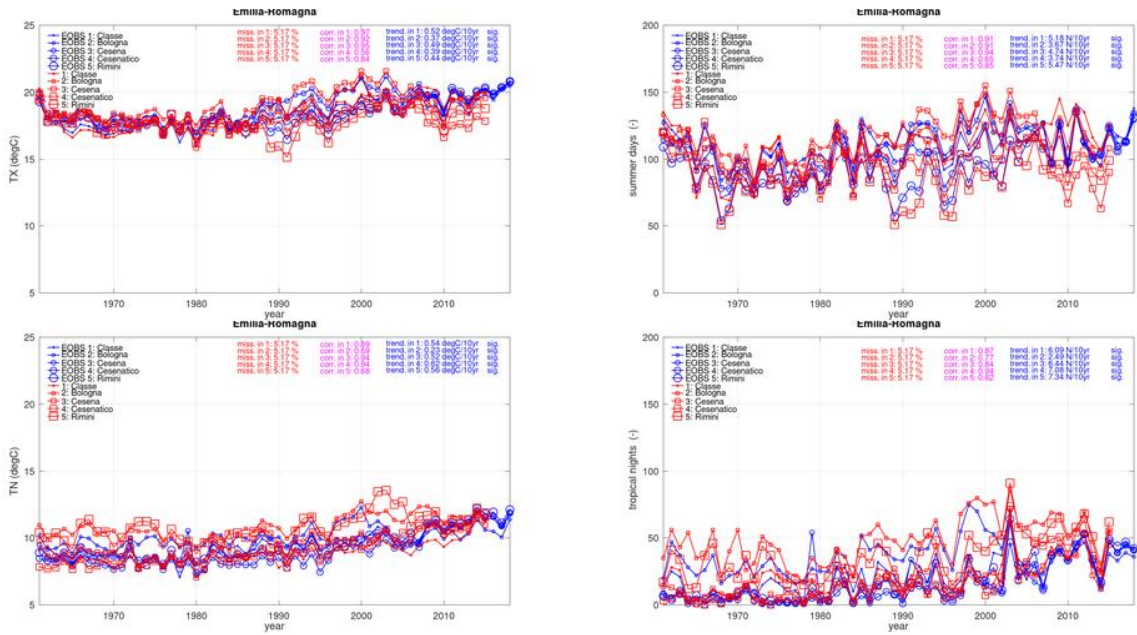


Figure 3.5 Same as Fig. 3.1 but for the selected six locations from the Italian region Veneto. Separate graphs for each location are available in Supplemental material to this deliverable.



**Figure 3.6** Same as Fig. 3.2 but for the selected six locations from the Italian region Veneto. Separate graphs for each location are available in Supplemental material to this deliverable.



**Figure 3.7** Same as Fig. 3.1 but for the selected five locations from the Italian region Emilia-Romagna. Separate graphs for each location are available in Supplemental material to this deliverable.

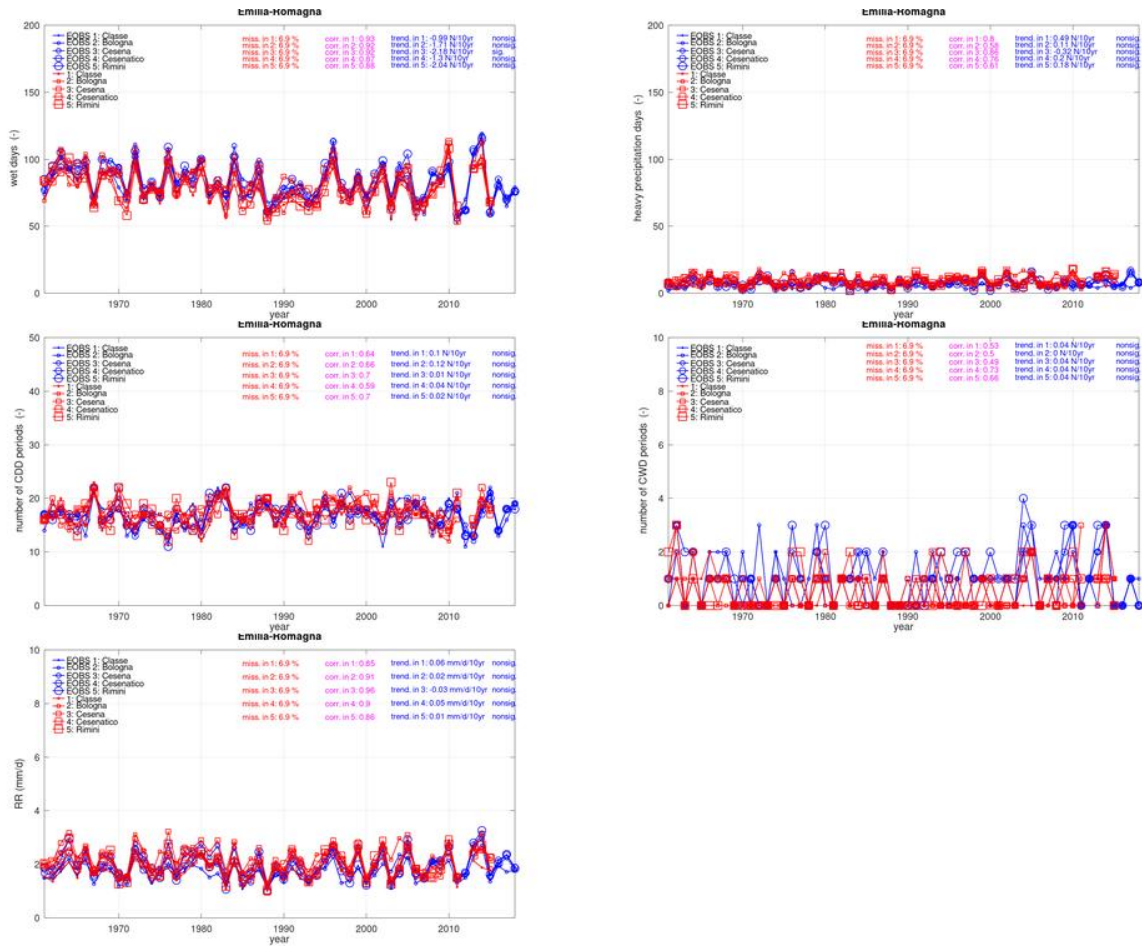


**Figure 3.8** Same as Fig. 3.2 but for the selected five locations from the Italian region Emilia-Romagna. Separate graphs for each location are available in Supplemental material to this deliverable.

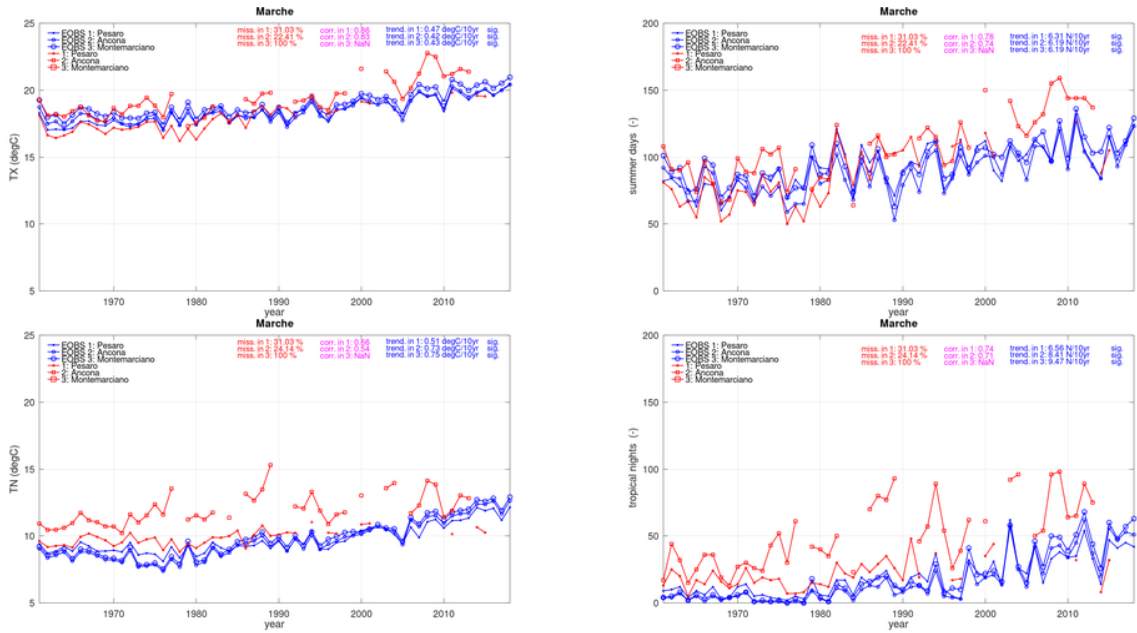


**Figure 3.9** Same as Fig. 3.1 but for the selected two locations from the Italian region Marche. Separate graphs for each location are available in Supplemental material to this deliverable.



**Figure 3.10** Same as Fig. 3.1 but for the selected two locations from the Italian region Marche. Separate graphs for each location are available in Supplemental material to this deliverable.

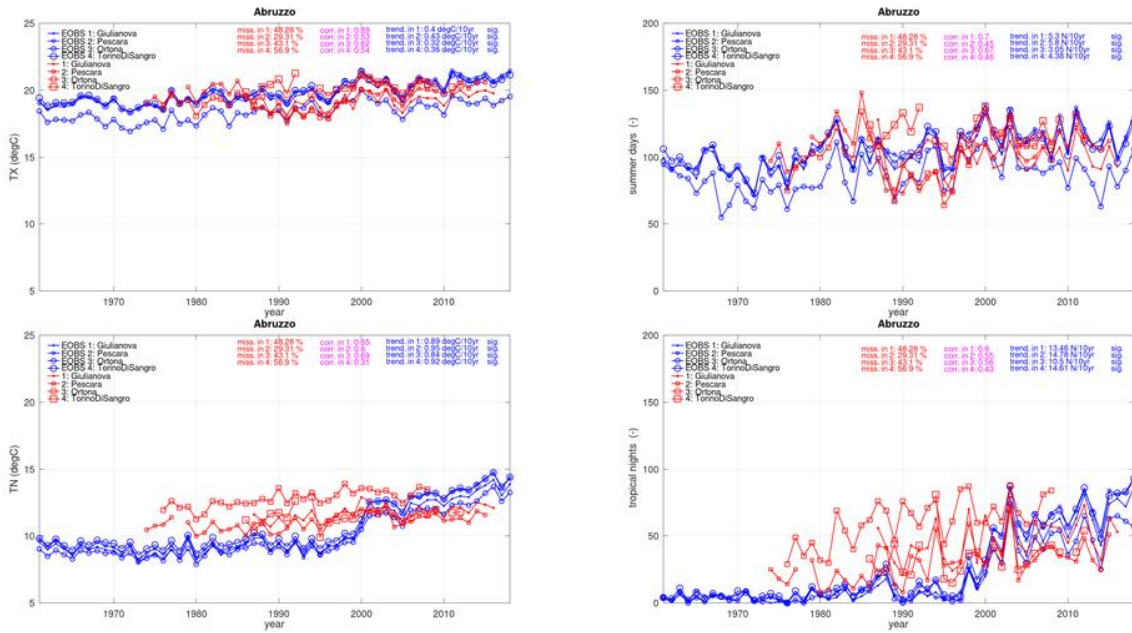


**Figure 3.11** Same as Fig. 3.1 but for the selected four locations from the Italian region Abruzzo. Separate graphs for each location are available in Supplemental material to this deliverable.

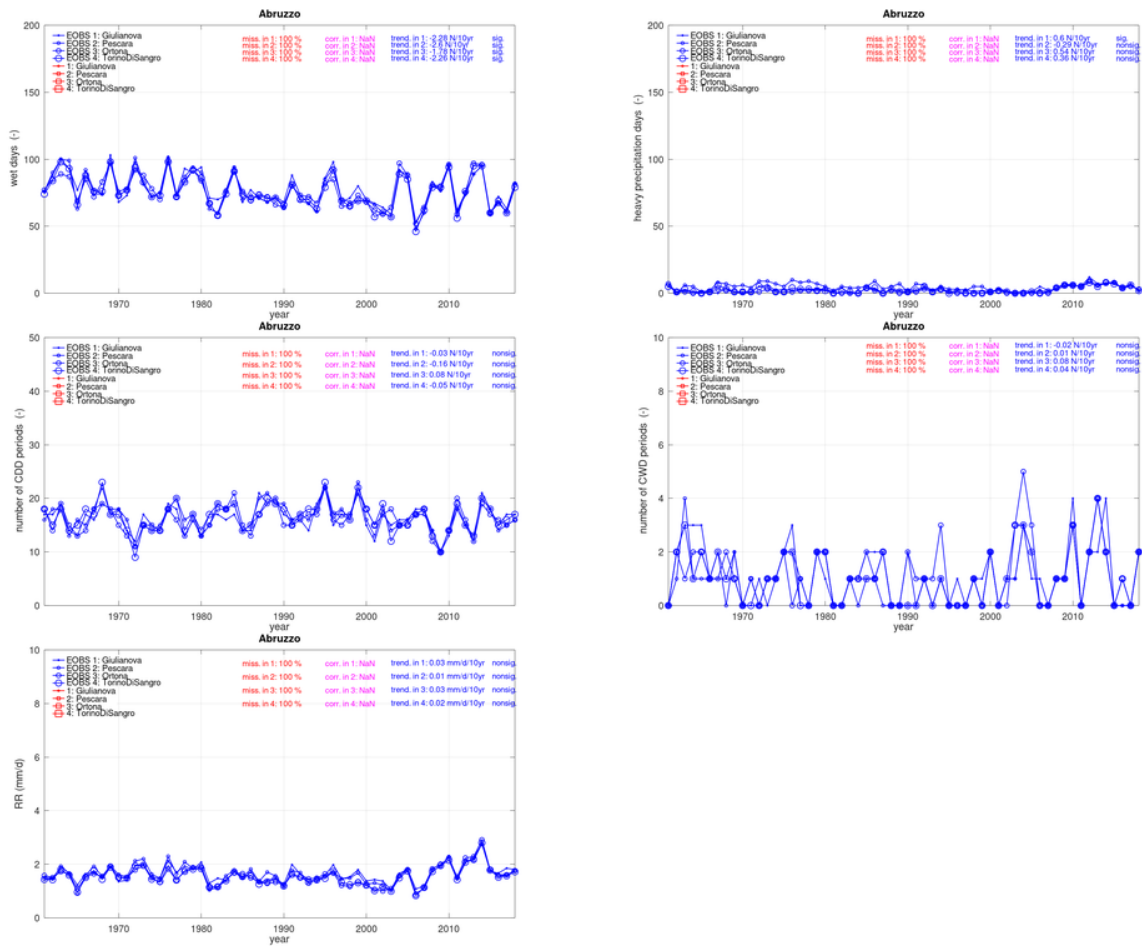


**Figure 3.12** Same as Fig. 3.2 but for the selected four locations from the Italian region Abruzzo. Separate graphs for each location are available in Supplemental material to this deliverable.

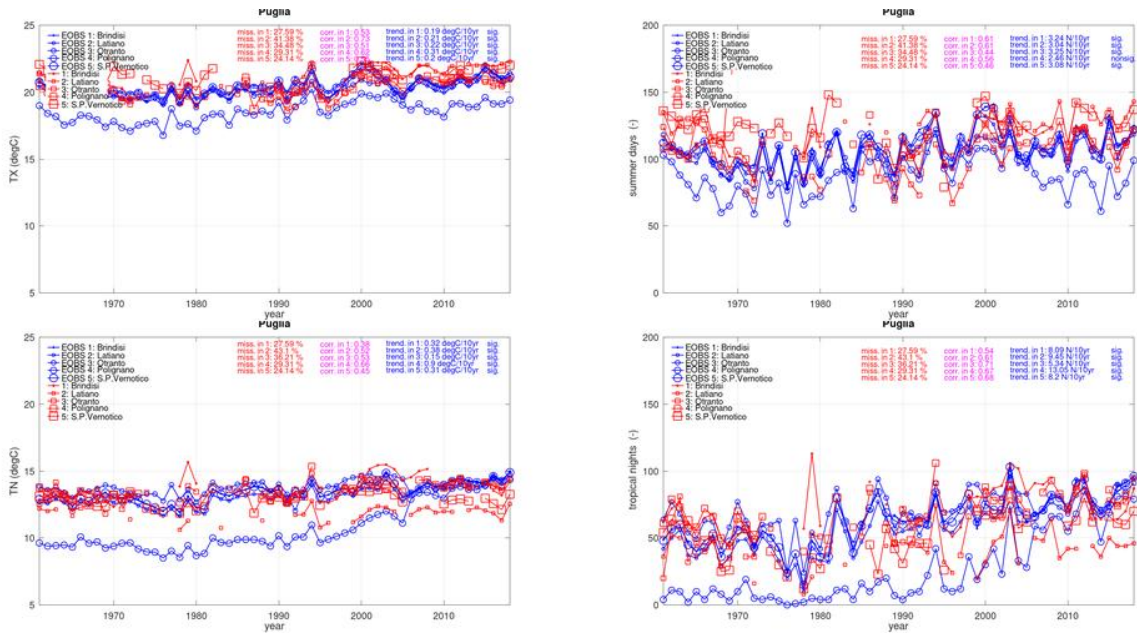


**Figure 3.13** Same as Fig. 3.1 but for the selected location from the Italian region Puglia. Separate graphs for each location are available in Supplemental material to this deliverable.

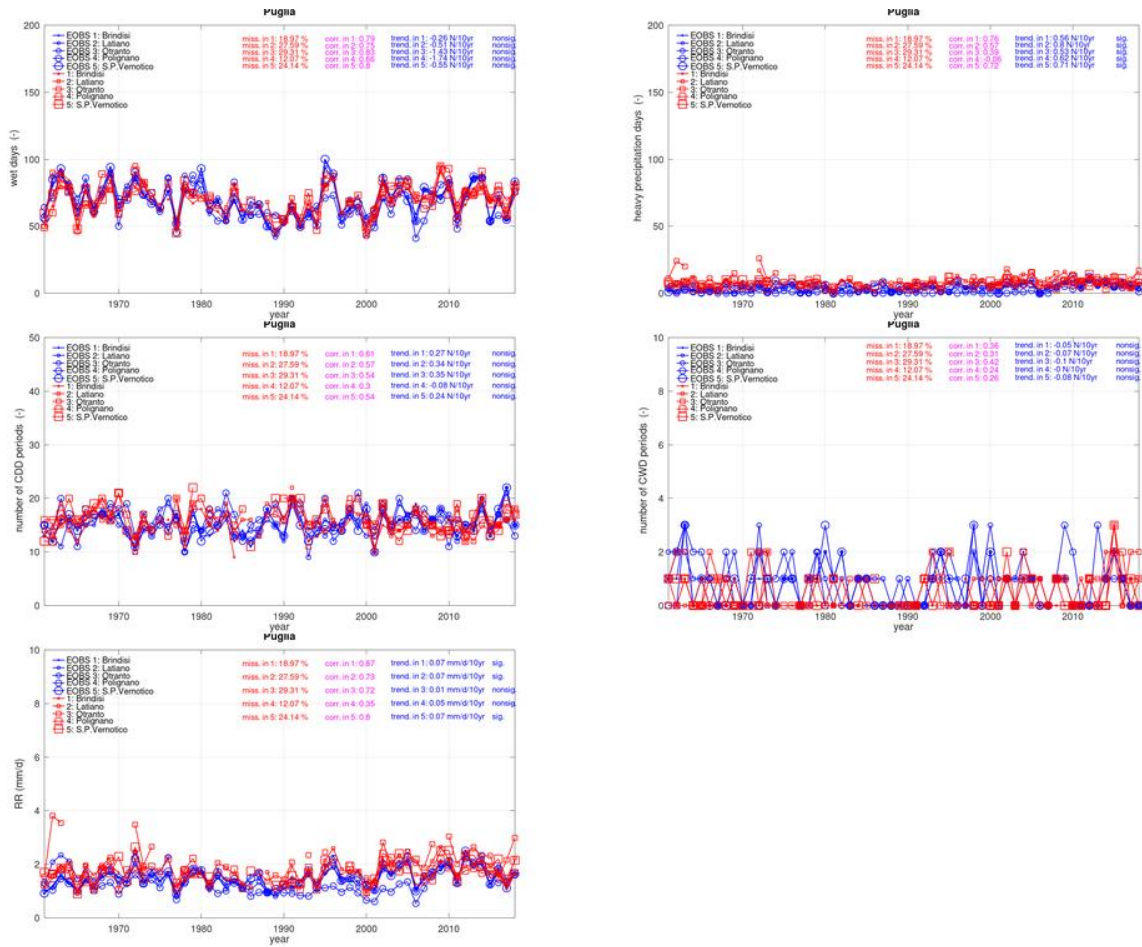


Figure 3.14 Same as Fig. 3.2 but for the selected location from the Italian region Puglia.

## 4 Examples of user targeted climate analysis

### CLIMATE INDEX FOR TOURISM

Adriatic area is very popular destination for holidays. As holidays and tourism are strongly modulated by weather and climate, climate index for tourism (CIT) was used to see what is the potential for different types of tourism at several destination along Adriatic coast.

Climate index for tourism was originally designed to rate the climate resource of beach tourism (so called 3S - sea, sand and sun tourism), De Freitas et al. (2009). It assesses daily weather asset by merging its thermal (T), aesthetic (A) and physical (P) facets. Bafaluy et al. (2014) modified the original 3S weather typology matrix to specifically rate different kinds of tourism, such as biking, hiking, golf, football, motor boating, sailing and cultural tourism.

CIT expresses the integrated body-atmosphere energy balance as a thermal sensation, taking into account physical activity and clothing insulation. Thermal component (T) in this report is calculated by using physiologically equivalent temperature PET (Höppe, 1999, Matzarakis et al. 1999). Calculation was done by RayMan model (Mazarakis et al. 1999) and meteorological variables temperature at 2 m, relative humidity, wind speed and cloudiness were used. As CIT do not rely only on thermal aspects, cloudiness as aesthetical and wind and precipitation as physical facets were used. CIT was calculated for two different parts of day, in the morning 7 am (i.e., 7 UTC) and early afternoon 2 pm (i.e., 14 UTC) for 30 year period 1981-2010, with the data obtained from ERA5 (C3S, 2017). CIT results can range from very poor tourism conditions (1 - unacceptable) to very good (7 - optimal) and to simplify discussion following categories are used: CIT= 1,2,3: unacceptable; CIT=4,5: acceptable and CIT=6,7 ideal conditions, respectively.

Conditions for different types of tourism differ during year as well as during the day. We provide CIT estimates for the following locations:

- (1) Lignano (IT) in Fig. 4.1.1.
- (2) Montemarignano (IT) in Fig. 4.1.2.
- (3) Brindisi (IT) in Fig. 4.1.3.
- (4) Cres (HR) in Fig. 4.1.4.
- (5) Šibenik (HR) in Fig. 4.1.5.
- (6) Dubrovnik (HR) in Fig. 4.1.6.

At 7 am 3S tourism has completely unacceptable conditions in cold part of the year (from November to March). In April and October acceptable conditions start to occur but with a probability of less than 20 %. Ideal conditions are present between May and September with the highest probability in July (they increase from north to the south at both sides of Adriatic and reach 58 % in Dubrovnik). During a day, at 2 pm, ideal conditions at some locations start already in April and they last till October. The highest probability of ideal conditions for 3S tourism is in July and August and can reach 71 % in Montemarignano.

Biking, hiking, golf, football and cultural tourism have similar distribution of categories. Unfavourable conditions in the cold part of the year prevail in the morning from November to February. Ideal conditions are present from April till October, with a very high probability greater than 80 % in July and August for all types except for golf. At 2 pm, the distribution of ideal conditions have a bimodal shape. Ideal conditions are slightly better in May and June and also in September and October in comparison with the warmest months (July and August).

The conditions for motor boating and sailing are very similar. Completely unacceptable conditions prevail for both types of activities from November to March at almost all locations at 7 am, whereas at 2 pm small probability of acceptable conditions is present in the same period. From May to September, during afternoon ideal conditions for motor boating and sailing are dominant.

It is noteworthy to observe that the results obtained with ERA5 are not always consistent with conditions encountered in real experience. For example, the real conditions found in Southern Italy at 2 pm are not suitable for playing football, especially in July and August. Such a difference could be ascribed to the limitations of ERA5 and similar products, already previously pointed out in this document.

Lignano

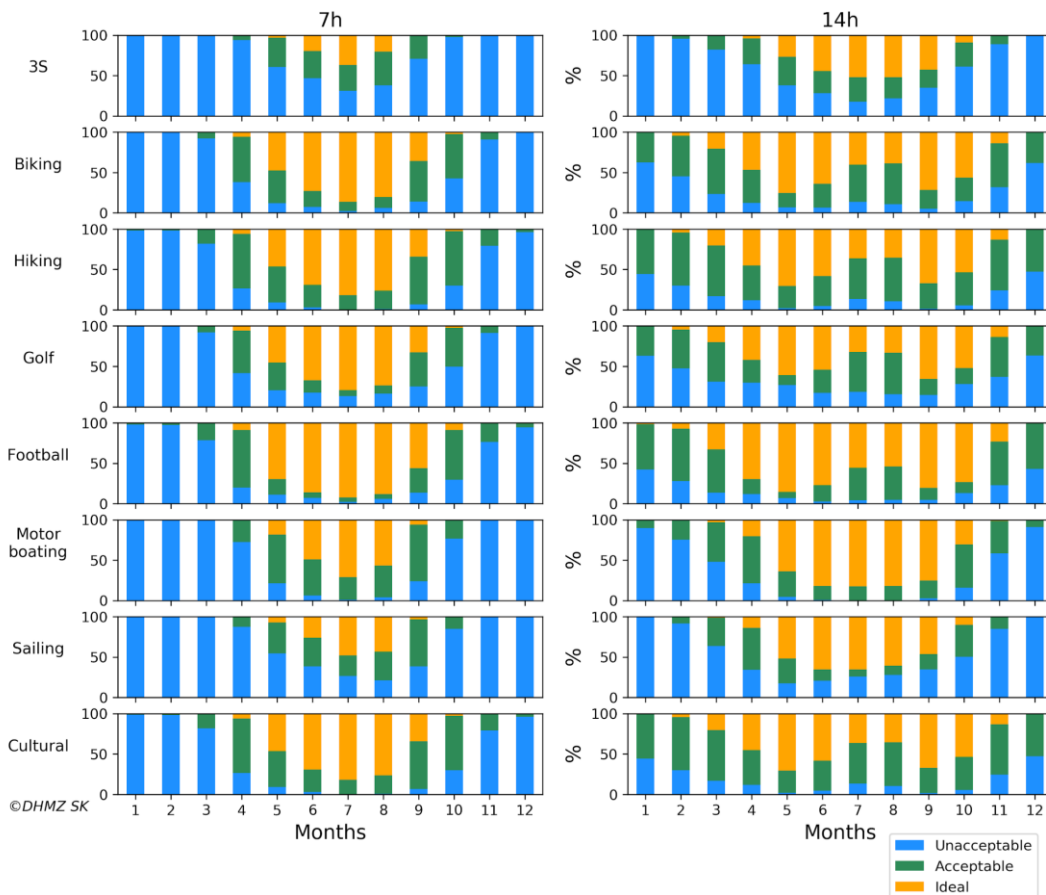


**Figure 4.1.1** Mean monthly frequency of conditions for specific tourism activity based on the Climate Index for Tourism for location of Lignano, based on the ERA5 reanalysis for the period 1981-2010, estimated at 7:00 and 14:00 UTC.

Montemarciano

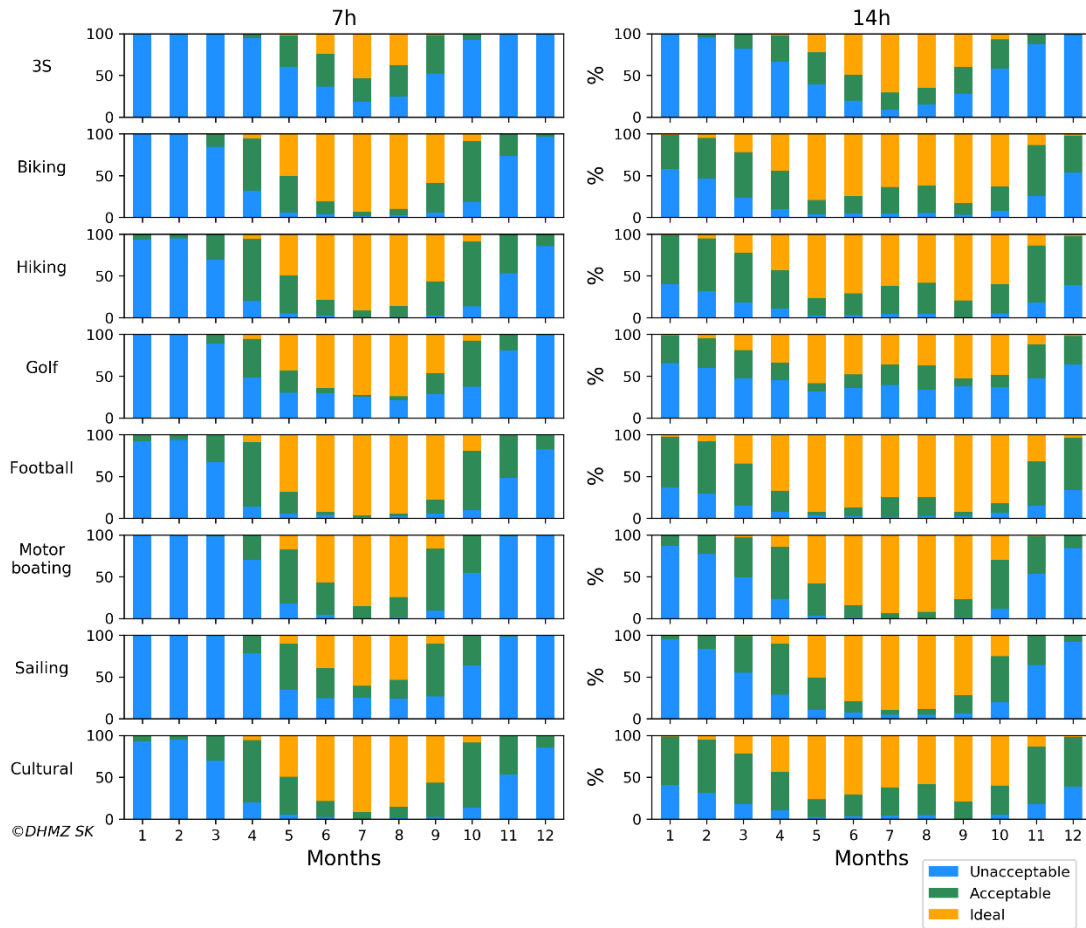


**Figure 4.1.2** Mean monthly frequency of conditions for specific tourism activity based on the Climate Index for Tourism for location of Montemarciano, based on the ERA5 reanalysis for the period 1981-2010, estimated at 7:00 and 14:00 UTC.

Brindisi

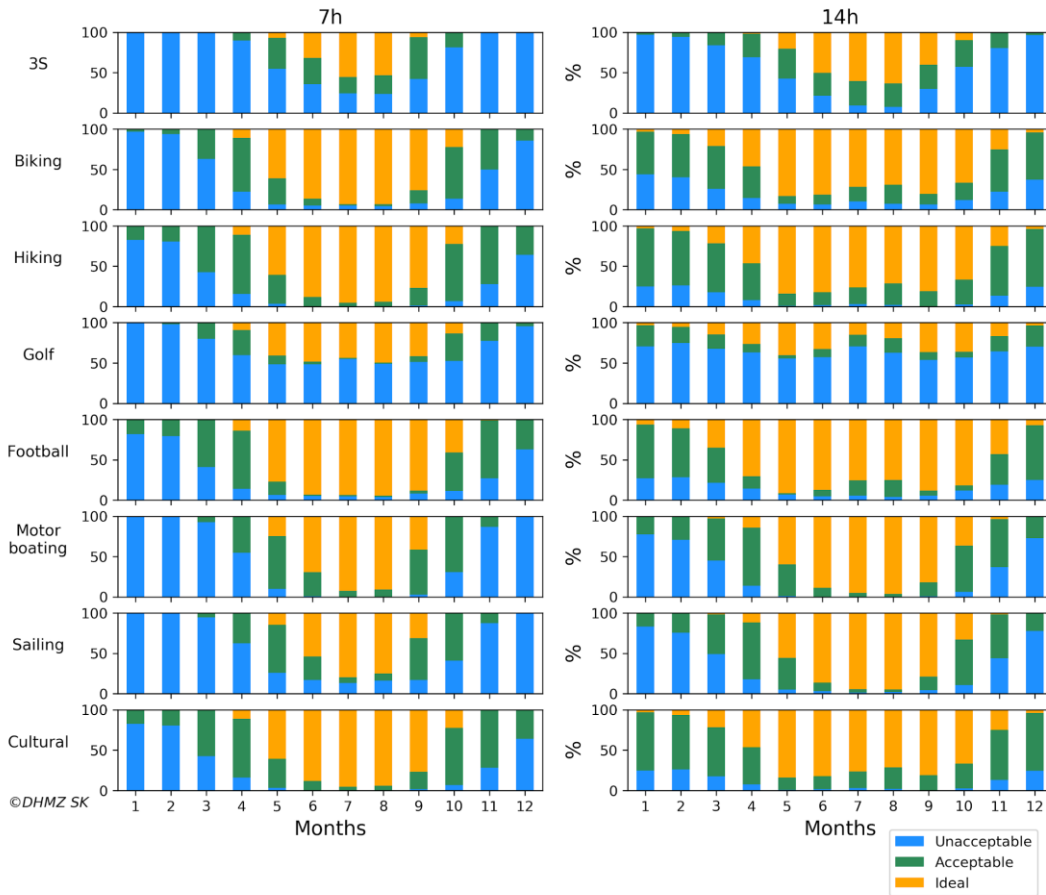


**Figure 4.1.3** Mean monthly frequency of conditions for specific tourism activity based on the Climate Index for Tourism for location of Brindisi, based on the ERA5 reanalysis for the period 1981-2010, estimated at 7:00 and 14:00 UTC.

Cres

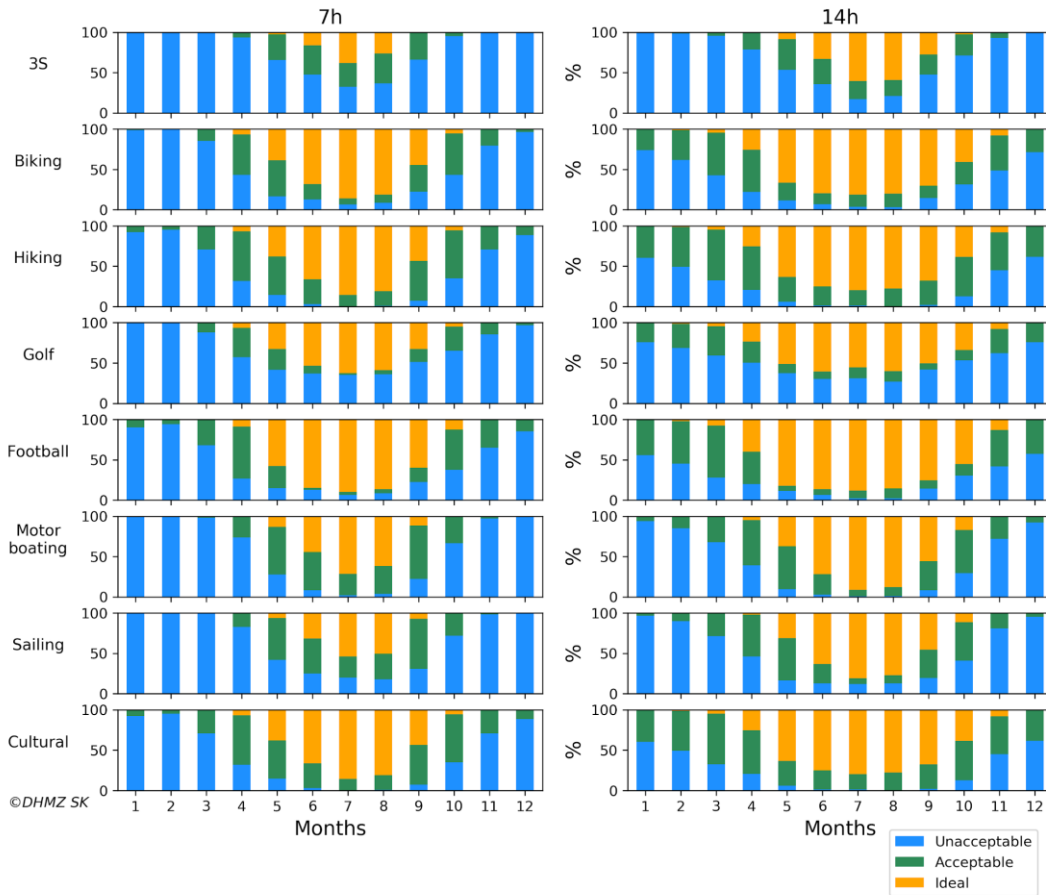


**Figure 4.1.4** Mean monthly frequency of conditions for specific tourism activity based on the Climate Index for Tourism for location of Cres, based on the ERA5 reanalysis for the period 1981-2010, estimated at 7:00 and 14:00 UTC.

Šibenik

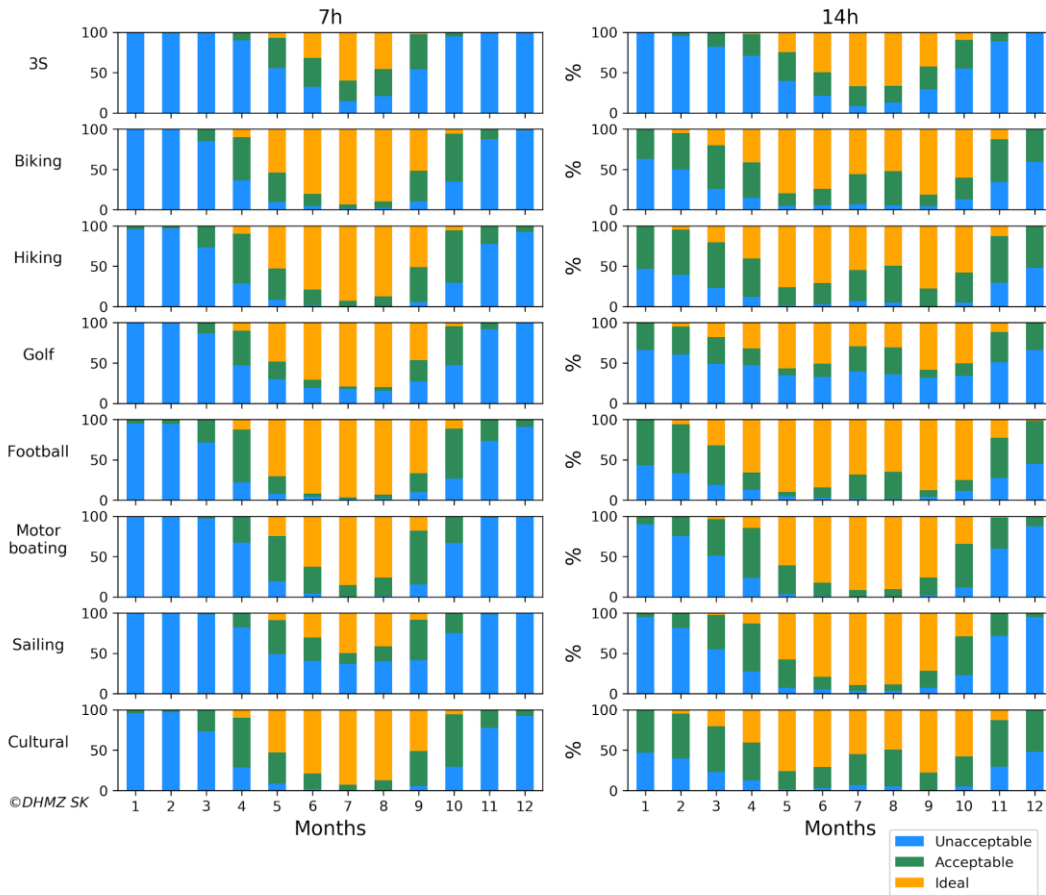


**Figure 4.1.5** Mean monthly frequency of conditions for specific tourism activity based on the Climate Index for Tourism for location of Šibenik, based on the ERA5 reanalysis for the period 1981-2010, estimated at 7:00 and 14:00 UTC.

Dubrovnik

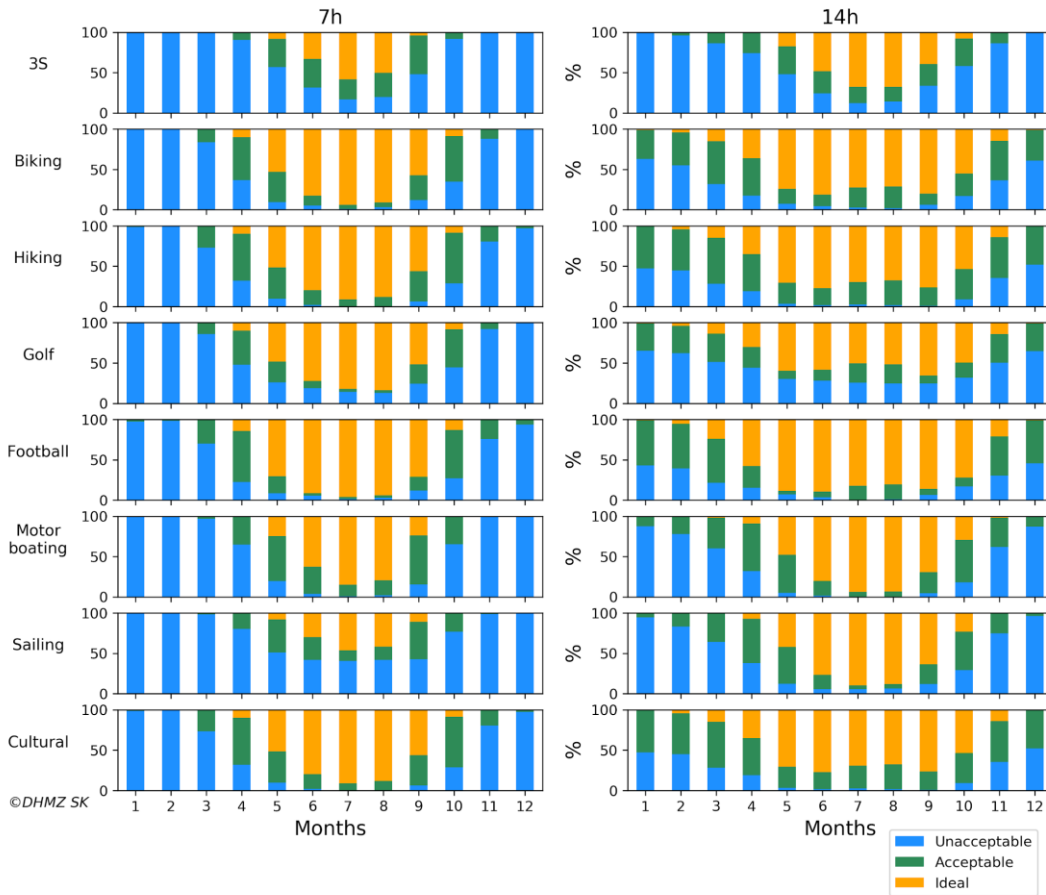


**Figure 4.1.6** Mean monthly frequency of conditions for specific tourism activity based on the Climate Index for Tourism for location of Dubrovnik, based on the ERA5 reanalysis for the period 1981-2010, estimated at 7:00 and 14:00 UTC.

## HEATING AND COOLING DEGREE DAYS

The degree-day method applied in this report is widely used to quantify the energy demand of buildings for heating and cooling. Basically, degree-days are defined as the differences between mean daily temperatures and a base temperature (threshold). The base temperature is the outdoor temperature below/above which a building is assumed to need heating/cooling. Therefore, energy requirements for heating and cooling become minimal around base temperatures.

**Heating degree day (HDD)** for the whole year period:

$$HDD = \sum_{i=1}^{365} m_i(T_{IN} - t_i), m_i=1 \text{ if } t_i < T_{OH}, \text{ and } m_i=0 \text{ if } t_i \geq T_{OH}$$

where  $t_i$  (°C) is the mean daily outdoor temperature of a particular day (i),  $T_{IN}$  (°C) is the desired indoor temperature, and  $T_{OH}$  (°C) is the outdoor temperature threshold. This study uses  $T_{IN} = 20$  °C and  $T_{OH} = 12$  °C.

**Cooling degree day (CDD)** for the whole year period:

$$CDD = \sum_{i=1}^{365} m_i(t_i - T_{OC}), m_i=1 \text{ if } t_i > T_{OC}, \text{ and } m_i=0 \text{ if } t_i \leq T_{OC}$$

where  $t_i$  (°C) is the mean daily outdoor temperature of a particular day (i), and  $T_{OC}$  (°C) is the outdoor temperature threshold. This study uses  $T_{OC} = 21$  °C.

The degree-day method assumes a linear relationship between energy demand and the degrees below (above) the heating (cooling) threshold (Cox et al., 2015). The larger (small) values of *HDD* and *CDD* imply larger (small) amounts of energy needed for heating and cooling. It is important to note that the desired indoor temperature ( $T_{IN}$ ) is usually defined for the heating season, while in the cooling season it is only recommended that the indoor temperature be no more than about 5 °C lower than the outdoor temperature on days when cooling is needed.

Analysed are annual values of *HDD* and *CDD* parameters over 1961-2018 period based on the E-OBS dataset (Cornes et al., 2018). We provide HDD and CDD harmonized analysis over six selected locations:

- (1) Lignano (IT) in Fig. 4.2.1.
- (2) Montemarciano (IT) in Fig. 4.2.2.
- (3) Brindisi (IT) in Fig. 4.2.3.
- (4) Cres (HR) in Fig. 4.2.4.
- (5) Šibenik (HR) in Fig. 4.2.5.
- (6) Dubrovnik (HR) in Fig. 4.2.6.

Decreasing trends in *HDD* and increasing trends in *CDD* are detected over the last 58 years at all six locations. All the trends are statistically significant and indicate a significant decline in the energy needed for heating and a significant increase in the energy needed for cooling.

Detected decreases of *HDD* annual values are undoubtedly financially convenient since they are connected with the decrease of heating energy demand, which is (over a century) as high as approximately 40% of appropriate average annual amount of heating energy demand at all three Croatian Adriatic locations, while ranges from 27% (Lignano Sabbiadoro) to 80% (Montemarignano) of appropriate average annual amount of heating energy demand at three locations in Italian Adriatic locations. These conclusions should be revisited using directly observed temperature when estimating *HDD*.

Trends in *CDD* are much more similar at the Croatian coast (1520°C/100years-1627°C/100years) than at the Italian side (969°C/100years-2666°C/100years). In comparison with mean annual *CDD* values in the period 1961–2018, the magnitudes of secular trends represent an increase in related mean *CDD* from 66% (Dubrovnik) to 104% (Cres) at the Croatian Adriatic side, and from 47% (Brindisi) to 143% (Montemarignano) at the Italian Adriatic side. The increasing *CDD* trends indicate the financially unfavourable fact of an increasing need for cooling energy. These conclusions should be revisited using directly observed temperature when estimating *CDD*.

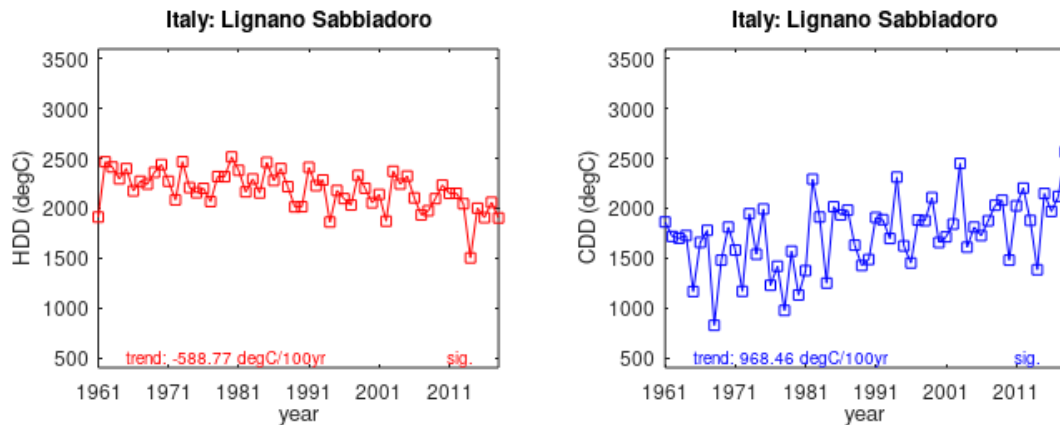


**Figure 4.2.1** Annual values of heating degree-days (*HDD*; left) and cooling degree-days (*CDD*; right) for the location of Lignano for the period 1961-2018 based on the E-OBS dataset. Linear trend and its statistical significance at the 5% significance level (based on the Man Kendall trend test) is provided.

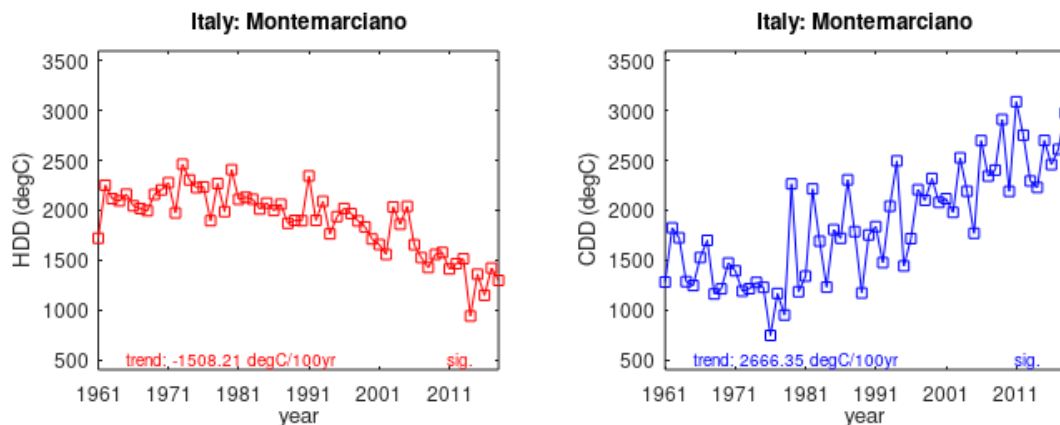


**Figure 4.2.2** Annual values of heating degree-days (*HDD*; left) and cooling degree-days (*CDD*; right) for the location of Montemarignano for the period 1961-2018 based on the E-OBS dataset. Linear trend and its statistical significance at the 5% significance level (based on the Man Kendall trend test) is provided.

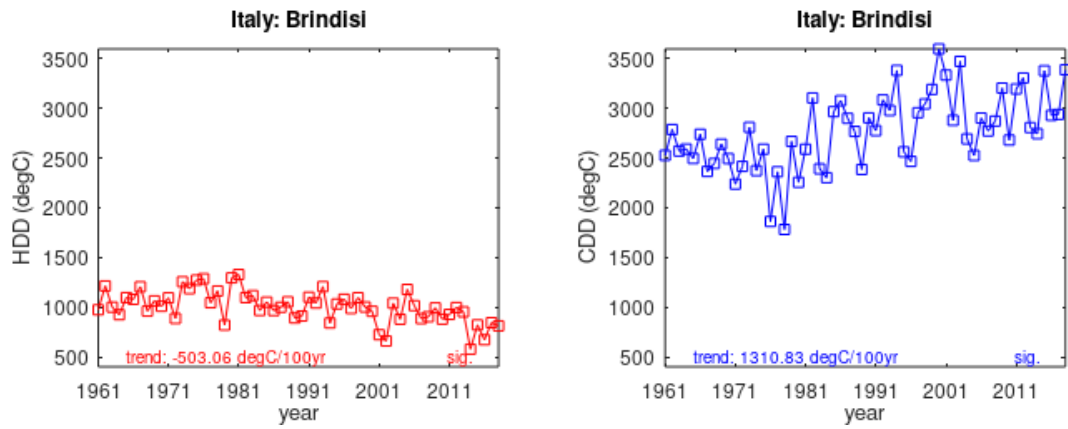


**Figure 4.2.3** Annual values of heating degree-days (*HDD*; left) and cooling degree-days (*CDD*; right) for the location of Brindisi for the period 1961-2018 based on the E-OBS dataset. Linear trend and its statistical significance at the 5% significance level (based on the Man Kendall trend test) is provided.

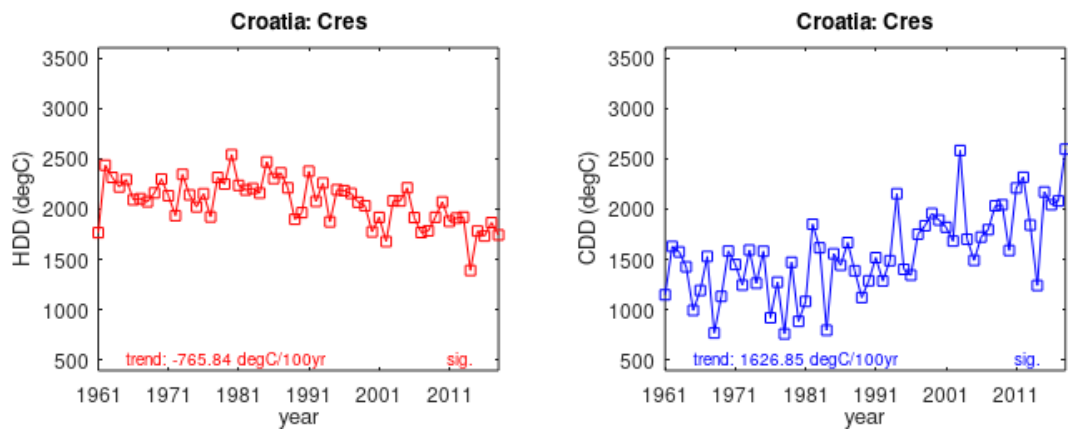


**Figure 4.2.4** Annual values of heating degree-days (*HDD*; left) and cooling degree-days (*CDD*; right) for the location of Cres for the period 1961-2018 based on the E-OBS dataset. Linear trend and its statistical significance at the 5% significance level (based on the Man Kendall trend test) is provided.

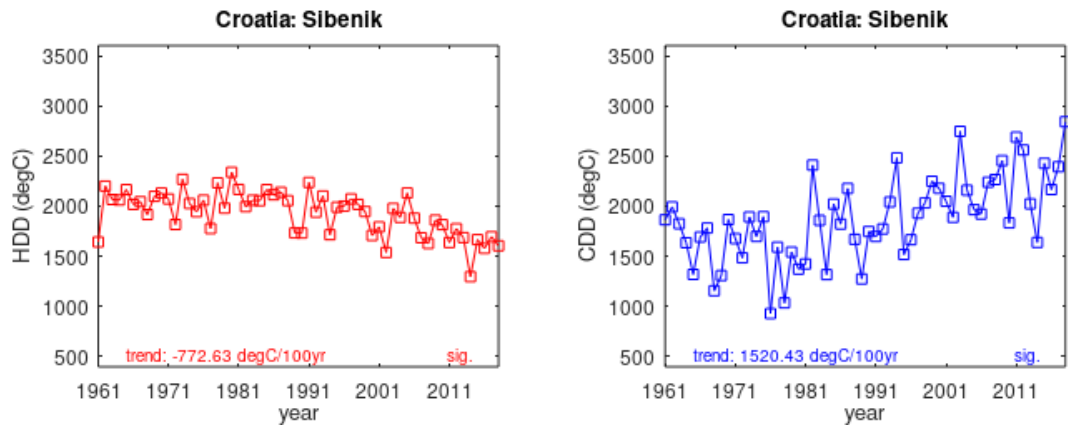


**Figure 4.2.5** Annual values of heating degree-days (*HDD*; left) and cooling degree-days (*CDD*; right) and for the location of Šibenik for the period 1961-2018 based on the E-OBS dataset. Linear trend and its statistical significance at the 5% significance level (based on the Man Kendall trend test) is provided.

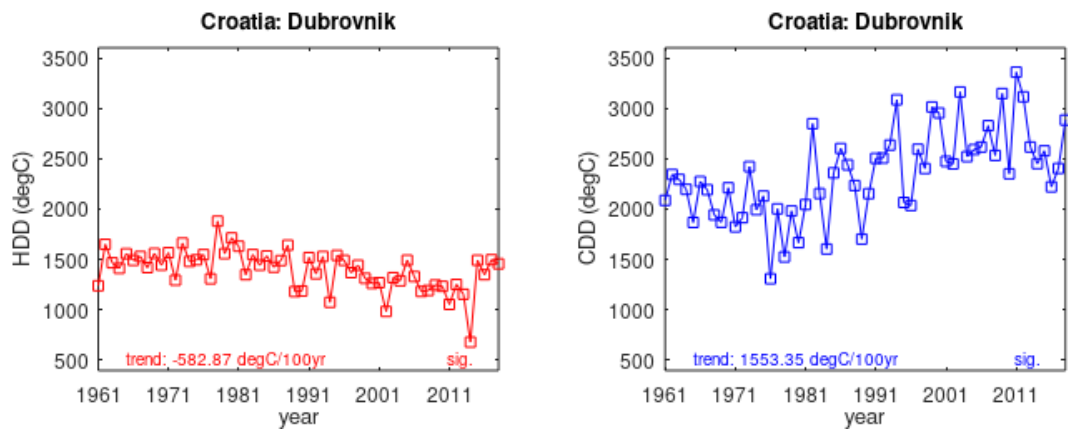


**Figure 4.2.6** Annual values of heating degree-days (*HDD*; left) and cooling degree-days (*CDD*; right) for the location of Dubrovnik for the period 1961-2018 based on the E-OBS dataset. Linear trend and its statistical significance at the 5% significance level (based on the Man Kendall trend test) is provided.

## EXTREME PRECIPITATION RETURN PERIODS

For six model focus locations (Italy: Lignano Sabbiadoro, Montemarciano, Brindisi; Croatia: Cres, Šibenik and Dubrovnik) we extract time-series of the daily precipitation from the E-OBS 19.0 dataset (<https://www.ecad.eu/download/ensembles/download.php#datafiles>; Cornes et al. 2018). For each year in the period from 1961 to 2018, maximum daily precipitation amount is determined, and using Generalized Extreme Value (GEV) theory, extreme precipitation amounts for the return periods 10, 20, 50, 100, 200, 500 and 1000 years are estimated. The results of this analysis are presented in Figs. 4.4.3.1 to 4.4.3.6. The largest values of almost 250 mm are found for the location of Dubrovnik and 1000-year return period based on the E-OBS datasets.

For a short introduction into the GEV theory and application please consider subsections 5.1 and 5.2 in the following deliverable of the EU Horizon 2020 project EU-CIRCLE: <http://www.eu-circle.eu/wp-content/uploads/2018/10/D3.2.pdf> and references therein.

The results present in this section are only indicative and should be revisited using high-quality local observations for the same period. Example is given for the Brindisi station where both local and E-OBS data are applied and analysed. Local observations show much larger annual maximum of the daily precipitation amounts in some of the years, leading to higher RR values for each specific return period. We provide GEV analysis for the following six locations:

- (1) Lignano (IT) in Fig. 4.3.1.
- (2) Montemarciano (IT) in Fig. 4.3.2.
- (3) Brindisi (IT) in Fig. 4.3.3.
- (4) Cres (HR) in Fig. 4.3.4.
- (5) Šibenik (HR) in Fig. 4.3.5.
- (6) Dubrovnik (HR) in Fig. 4.3.6.

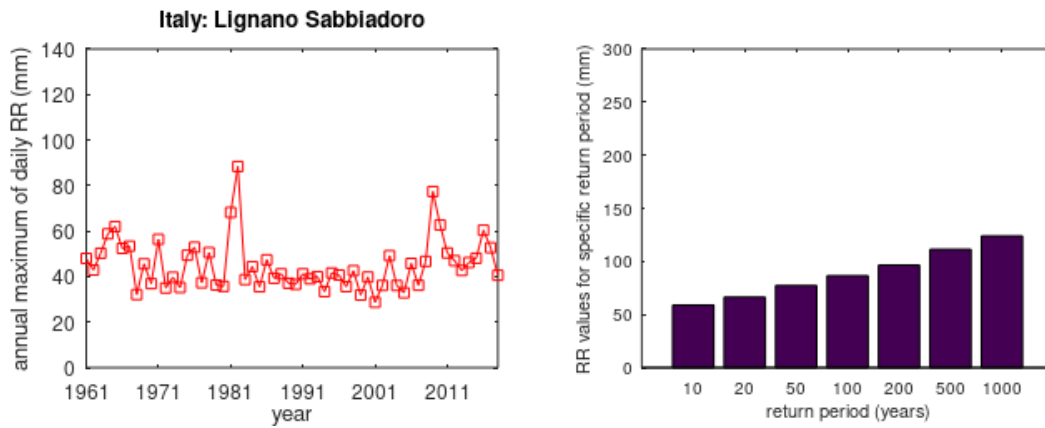


**Figure 4.3.1** Time series of the maximum annual daily precipitation amount for the location Lignano for the period 1961-2018 based on the E-OBS dataset (left). Estimations of the extreme precipitation amounts for the return period of 10, 20, 50, 100, 200, 500 and 1000 years (right) using the Generalized Extreme Value method.

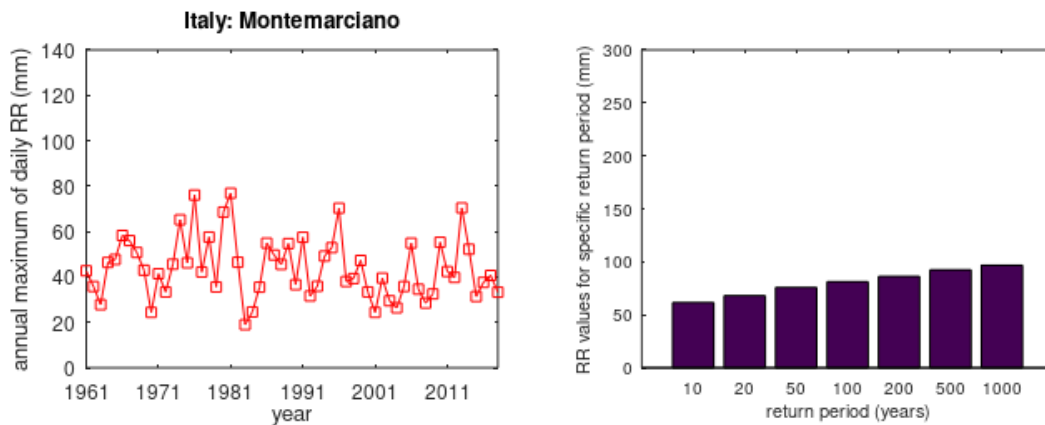


**Figure 4.3.2** Time series of the maximum annual daily precipitation amount for the location Montemarciano for the period 1961-2018 based on the E-OBS dataset (left). Estimations of the extreme precipitation amounts for the return period of 10, 20, 50, 100, 200, 500 and 1000 years (right) using the Generalized Extreme Value method.

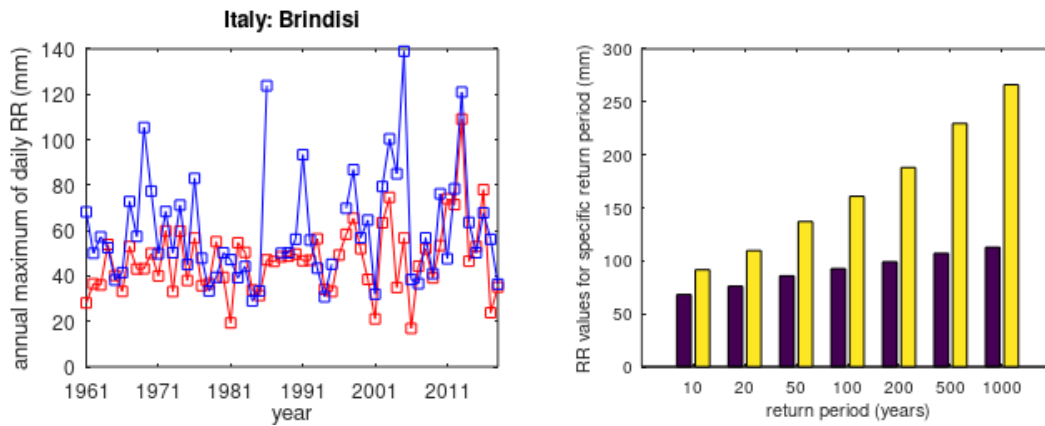


**Figure 4.3.3** Time series of the maximum annual daily precipitation amount for the location Brindisi for the period 1961-2018 based on the E-OBS dataset (left; red) and local observations (left; blue). Estimations of the extreme precipitation amounts for the return period of 10, 20, 50, 100, 200, 500 and 1000 years (right) using the Generalized Extreme Value method (blue: E-OBS, yellow: local observations).

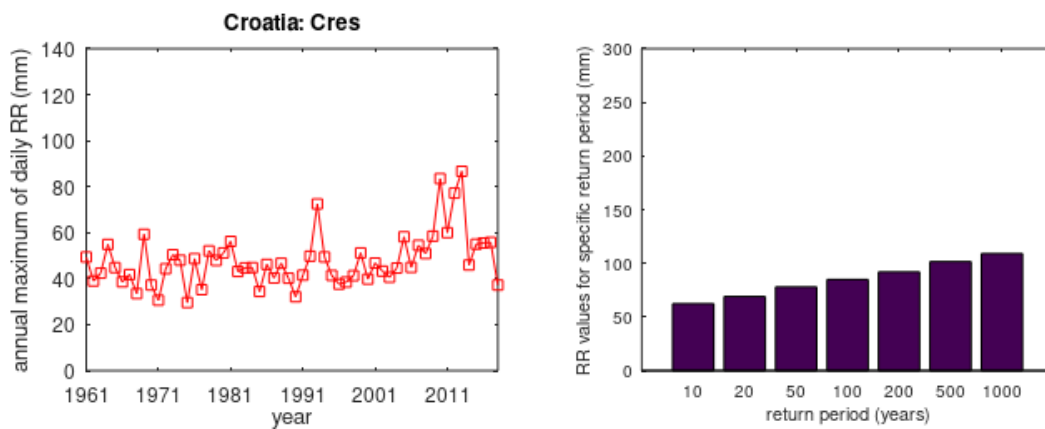


**Figure 4.3.4** Time series of the maximum annual daily precipitation amount for the location Cres for the period 1961-2018 based on the E-OBS dataset (left). Estimations of the extreme precipitation amounts for the return period of 10, 20, 50, 100, 200, 500 and 1000 years (right) using the Generalized Extreme Value method.

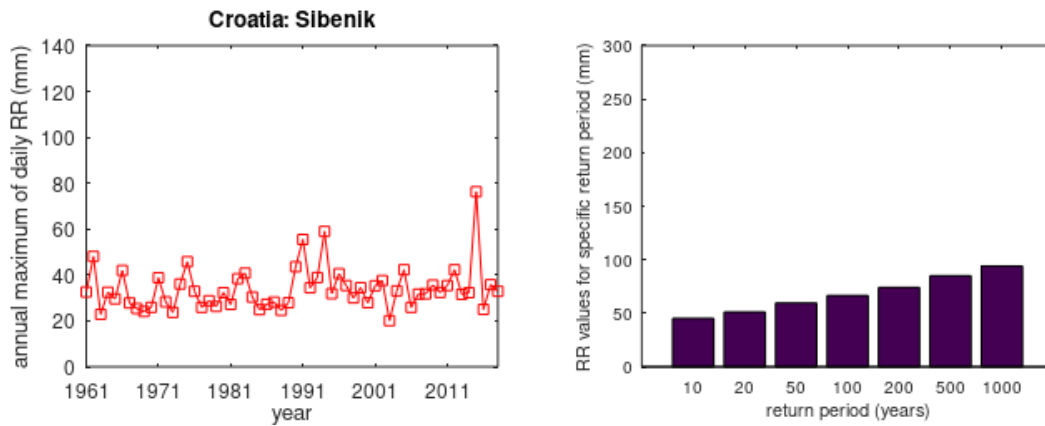


**Figure 4.3.5** Time series of the maximum annual daily precipitation amount for the location Šibenik for the period 1961-2018 based on the E-OBS dataset (left). Estimations of the extreme precipitation amounts for the return period of 10, 20, 50, 100, 200, 500 and 1000 years (right) using the Generalized Extreme Value method.

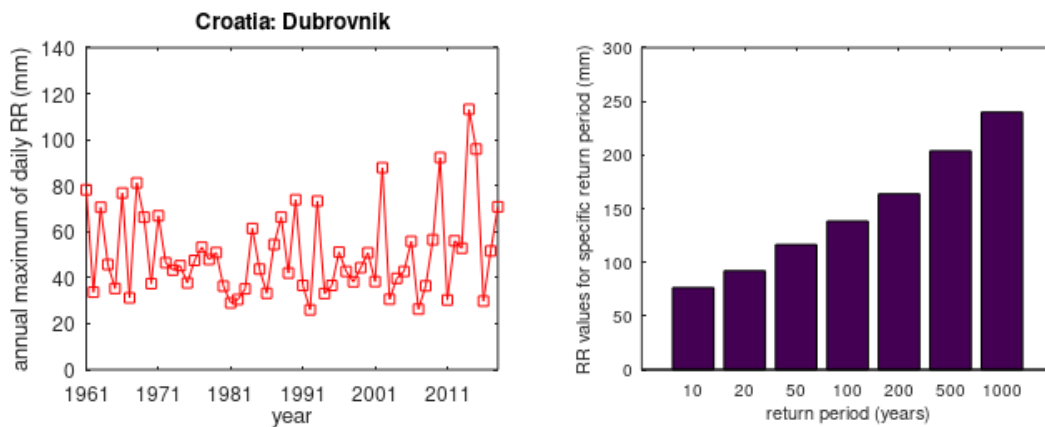


**Figure 4.3.6** Time series of the maximum annual daily precipitation amount for the location Dubrovnik for the period 1961-2018 based on the E-OBS dataset (left). Estimations of the extreme precipitation amounts for the return period of 10, 20, 50, 100, 200, 500 and 1000 years (right) using the Generalized Extreme Value method.

## WIND SPEED AND WIND GUSTS TRENDS

For six model focus locations (Italy: Lignano Sabbiadoro, Montemarciano, Brindisi; Croatia: Cres, Šibenik and Dubrovnik) we extract time series of the 1-hourly 10 m wind speed magnitude and wind gust from the ERA5 reanalysis (<https://www.ecmwf.int/en/forecasts/datasets/reanalysis-datasets/era5>; C3S, 2017 ). For each year in the period from 1979 to 2018, annual mean and maximum values are determined, with linear trend of the specific annual-based time series added. The results of this analysis are presented in Figs. 4.4.1 to 4.4.6. Following results are found: **(1)** increase (*decrease*) of the mean (*maximum*) annual wind speed and wind gusts for locations of Lignano Sabiaddoro, Brindisi, Šibenik and Dubrovnik, and **(2)** increase (*decrease*) of the both annual mean and maximum of the wind speed (*wind gusts*) for Montemarciano and Cres according to the ERA5 reanalysis.

The results present in this section are only indicative and should be revisited using high-quality local observations for the same period.

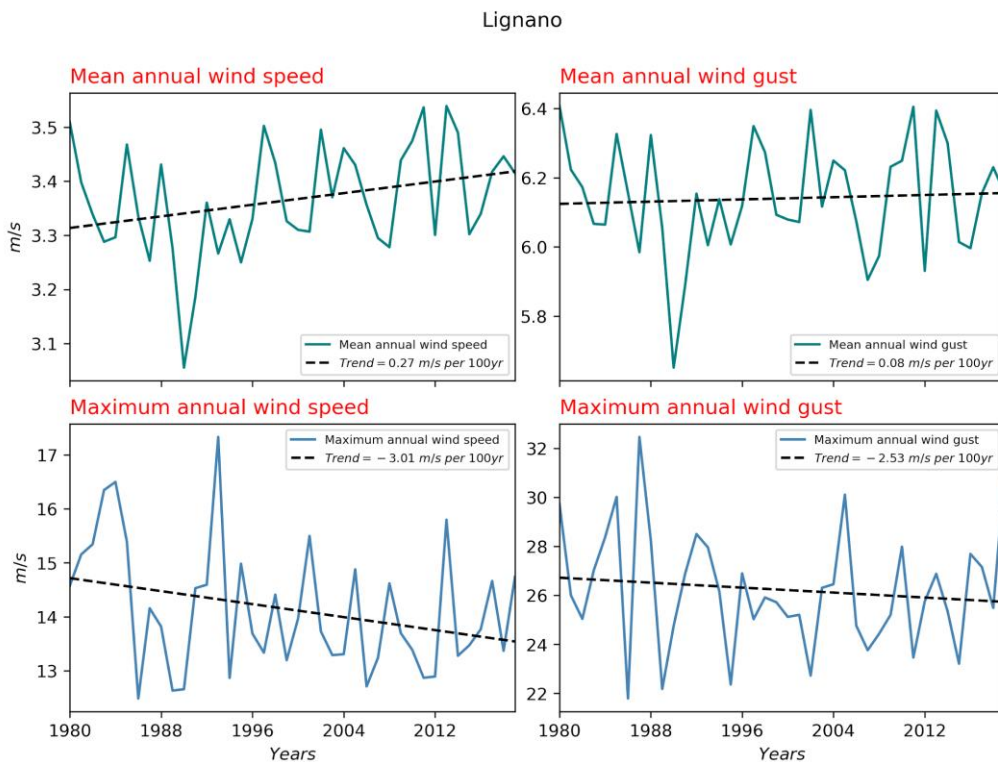


**Figure 4.4.1** Time series of the mean annual wind speed and mean annual wind gust (first row) and maximum annual wind speed and maximum annual wind gust (second row) based on the 1-hourly output of the ERA5 reanalysis for the location Lignano for the period 1979-2018.

Montemarciano

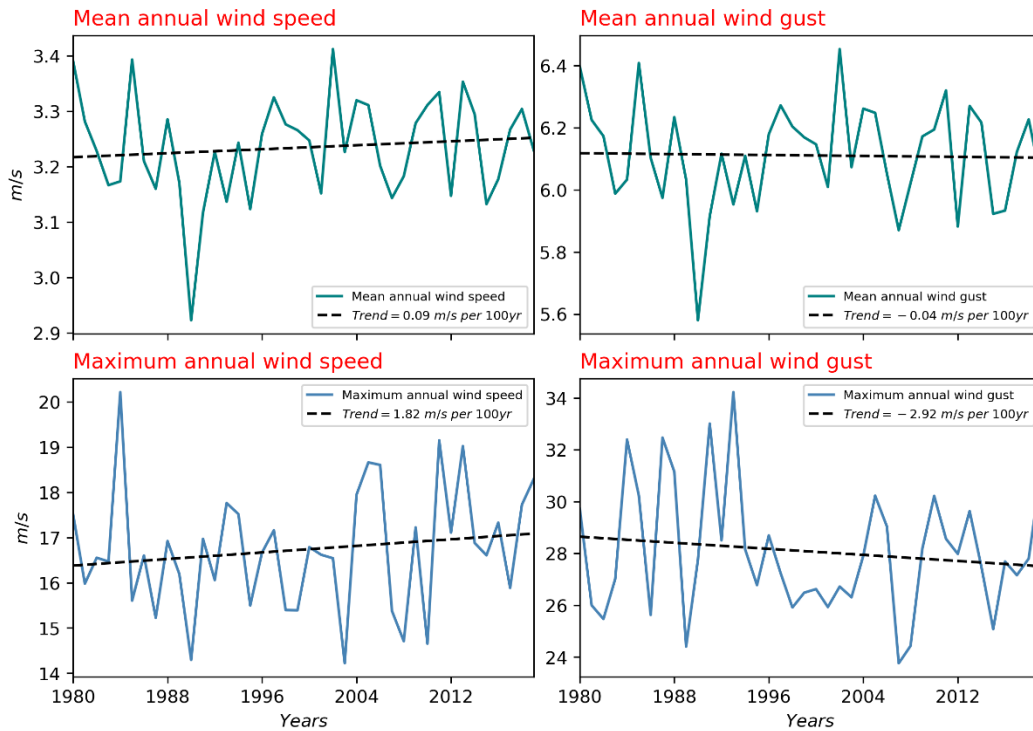


**Figure 4.4.2** Time series of the mean annual wind speed and mean annual wind gust (first row) and maximum annual wind speed and maximum annual wind gust (second row) based on the 1-hourly output of the ERA5 reanalysis for the location Montemarciano for the period 1979-2018.

Brindisi

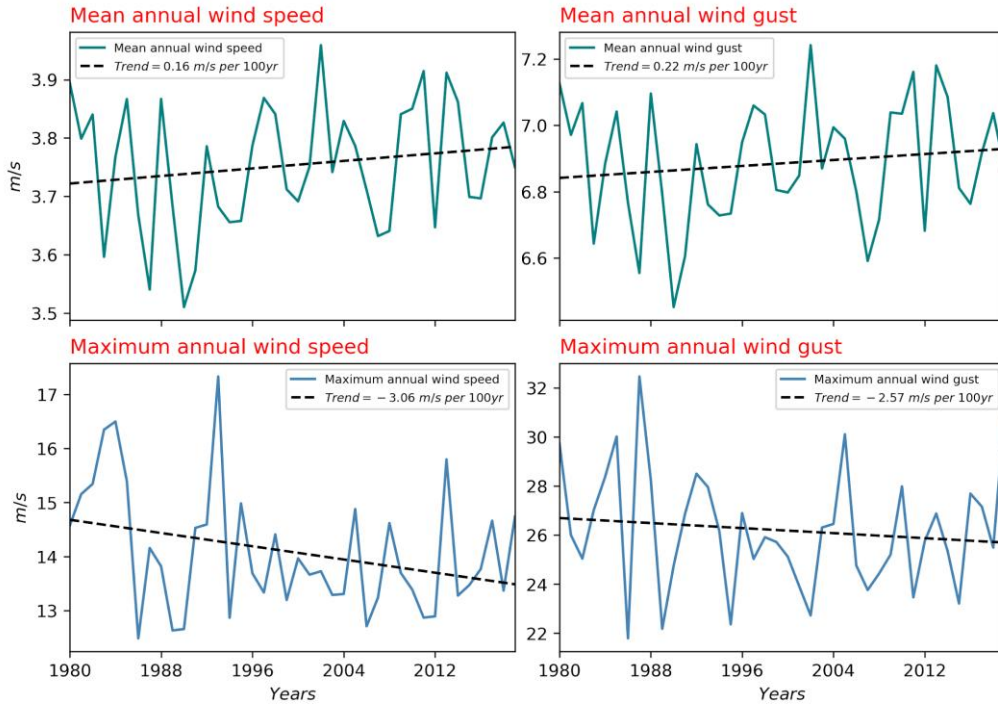


**Figure 4.4.3** Time series of the mean annual wind speed and mean annual wind gust (first row) and maximum annual wind speed and maximum annual wind gust (second row) based on the 1-hourly output of the ERA5 reanalysis for the location Brindisi for the period 1979-2018.

Cres

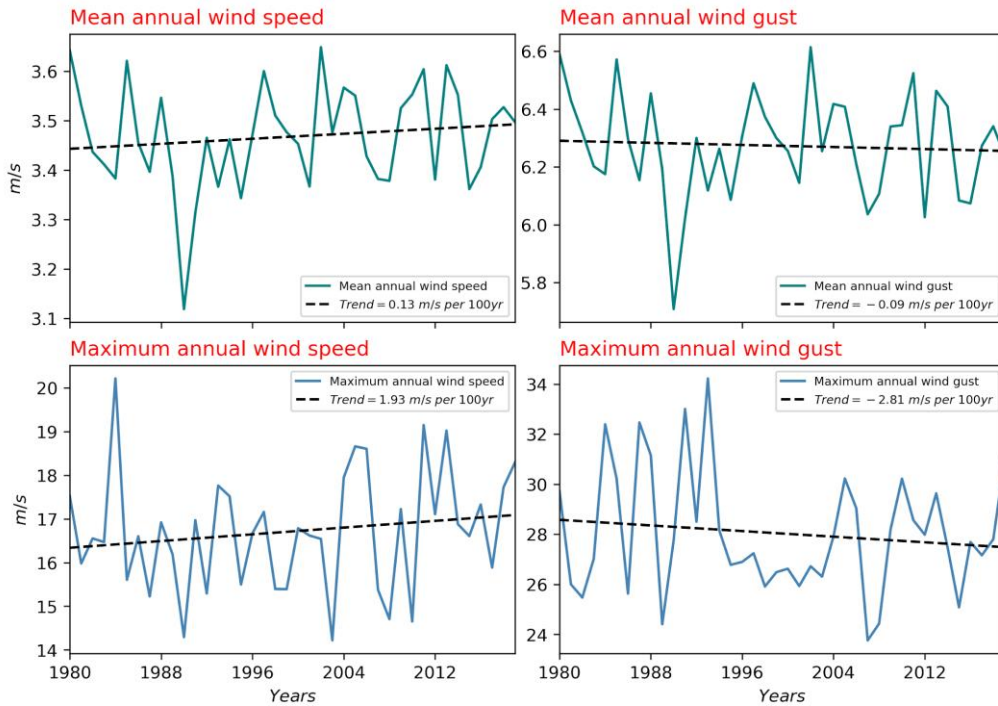


**Figure 4.4.4** Time series of the mean annual wind speed and mean annual wind gust (first row) and maximum annual wind speed and maximum annual wind gust (second row) based on the 1-hourly output of the ERA5 reanalysis for the location Cres for the period 1979-2018.

Šibenik

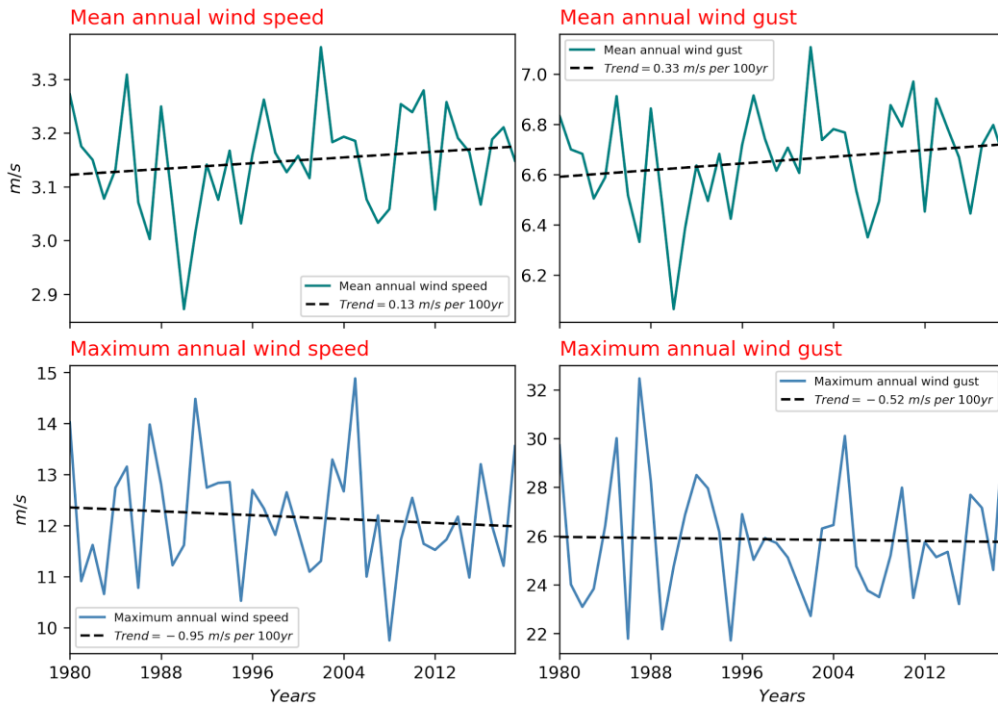


**Figure 4.4.5** Time series of the mean annual wind speed and mean annual wind gust (first row) and maximum annual wind speed and maximum annual wind gust (second row) based on the 1-hourly output of the ERA5 reanalysis for the location Šibenik for the period 1979-2018.

Dubrovnik

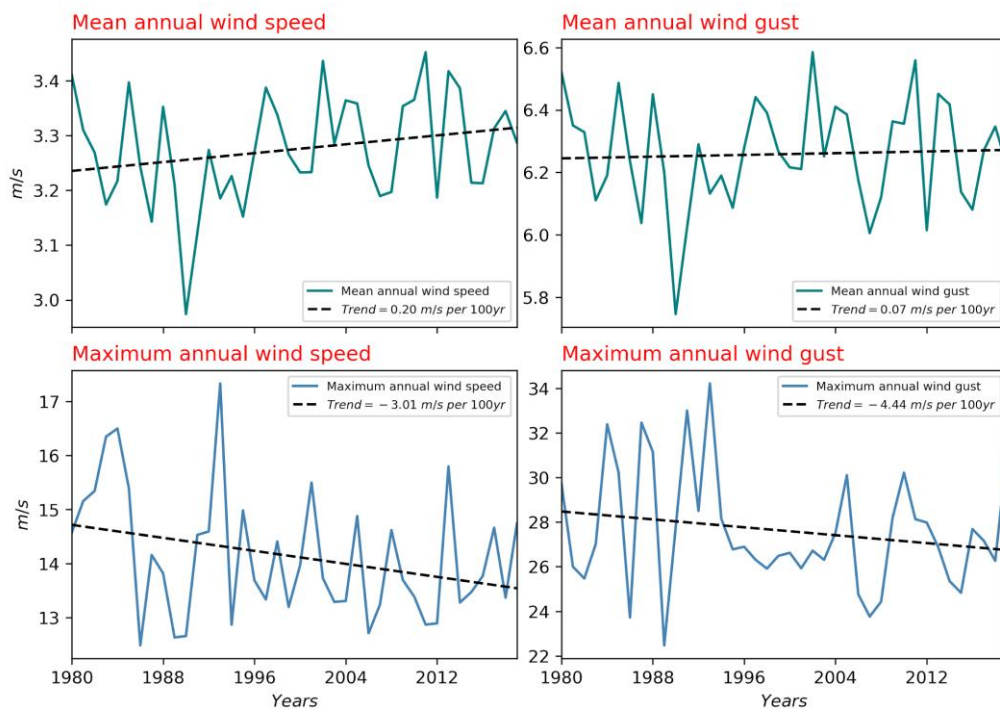


**Figure 4.4.6** Time series of the mean annual wind speed and mean annual wind gust (first row) and maximum annual wind speed and maximum annual wind gust (second row) based on the 1-hourly output of the ERA5 reanalysis for the location Dubrovnik for the period 1979-2018.

## 5 Sea temperature trends in the Adriatic

### INTRODUCTION

The Adriatic Sea has long been recognized as the sea sensitive to climate changes. Large-scale atmospheric pattern affects the marine surface layers through regional weather pattern and ocean features. Natural modes of atmospheric variability such as the North Atlantic Oscillation (NAO), Arctic Oscillation (AO) and Mediterranean Oscillation (MO) during winter impose changes in the wind stress and heat flux on the ocean causing changes of temperature and salinity at the surface layer (Grbec et al., 2007; Matic et al., 2011; Grbec et al., 2009). In this boundary layer, sea surface temperature (SST) is a parameter that controls feedback processes so it is reasonable to use it as a climate indicator due to the simplicity of its measurement and accessibility of data, either from coastal stations, oceanographic cruises or obtained by satellite. SST is a convenient starting point for the interdisciplinary research of air-sea interaction and marine ecosystems. In the Adriatic Sea, temperature conditions have been the subject of investigation since Lorenz (1863), though the analysis of daily SST measured at coastal stations of the eastern Adriatic is limited. Annual and seasonal properties of SST time-series obtained by coastal stations measurements can be found in Zore-Armanda (1969). Supić and Orlić (1992) documented year-to-year sea surface temperature variations in the period 1960–1980 measured at 21 stations along the Croatian coast, and investigated their variability using Fourier analysis. They found a cooling trend throughout the eastern Adriatic coast, which was more pronounced in the south than in the north Adriatic. Since 1980, a positive SST trend has been observed in the open Adriatic (Vilibić et al. 2013). Grbec, et al. (2018) documented the long-term in situ SST variations and trends along the eastern Adriatic, and their connection to hemispheric patterns using trend and multivariate analyses and Self-Organising Maps clustering. Throughout the year sea surface temperature in the Adriatic Sea is highly variable and clearly show the existence of four seasons, contrary to the eastern and western Mediterranean, where only two main patterns are evidenced. Based on the earlier investigations (Grbec, 1997, Grbec, et al., 2006) the sea surface temperature of the EAS is controlled mainly by vertical exchanges processes at the air-sea boundary. From April to September the sea is receiving heat from the atmosphere, reaching maximum in July. Maximal heat loss occurs in December. On the annual scale the heat loss is caused by long-wave radiation (60%), evaporation (33%) and by conduction (7%) (Grbec and Morović, 1997).

### DATA AND METHOD

Sea surface temperature (SST) data were collected by the Marine Meteorological Service of the Croatian Meteorological and Hydrological Service (MMS/DHMZ) along the eastern Adriatic coast since 1959. In situ SST was measured three times a day (7, 14 and 21 h) using a bucket thermometer, at a depth of 30 cm in water deeper than 1.8 m, following the guidelines of the World Meteorological Organization (WMO). The longest series were collected at Senj and Hvar (since 1964), Rab (since 1961) and Split (since 1959). The Split station moved its location by about 2.5 km in 1979/1980, yet the series were tested for homogeneity. At all locations, SST was measured without changing observational procedures. The data were averaged, and monthly and yearly-averaged SST values were used for trend analysis. In addition to the in situ coastal SST measurements, we used in situ SST data collected by the Institute of Oceanography and Fisheries (IOF) during oceanographic cruises at Stončica station (Figure 5.1), surveyed quasi-regularly on a monthly basis since 1961. As SSTs were measured once per month, the monthly dataset is therefore

represented, in most cases, by a single value. Detailed description of sea temperature measurements at Stončica station can be found in Zore-Armanda et al. (1991), Grbec and Morović (1997) and Grbec (1997). For the RESPONSE project we used and analyses data collected in the Adriatic Sea at permanent stations Senj, Rab, Split, Hvar, and at ocean station Stončica, located near Vis island.

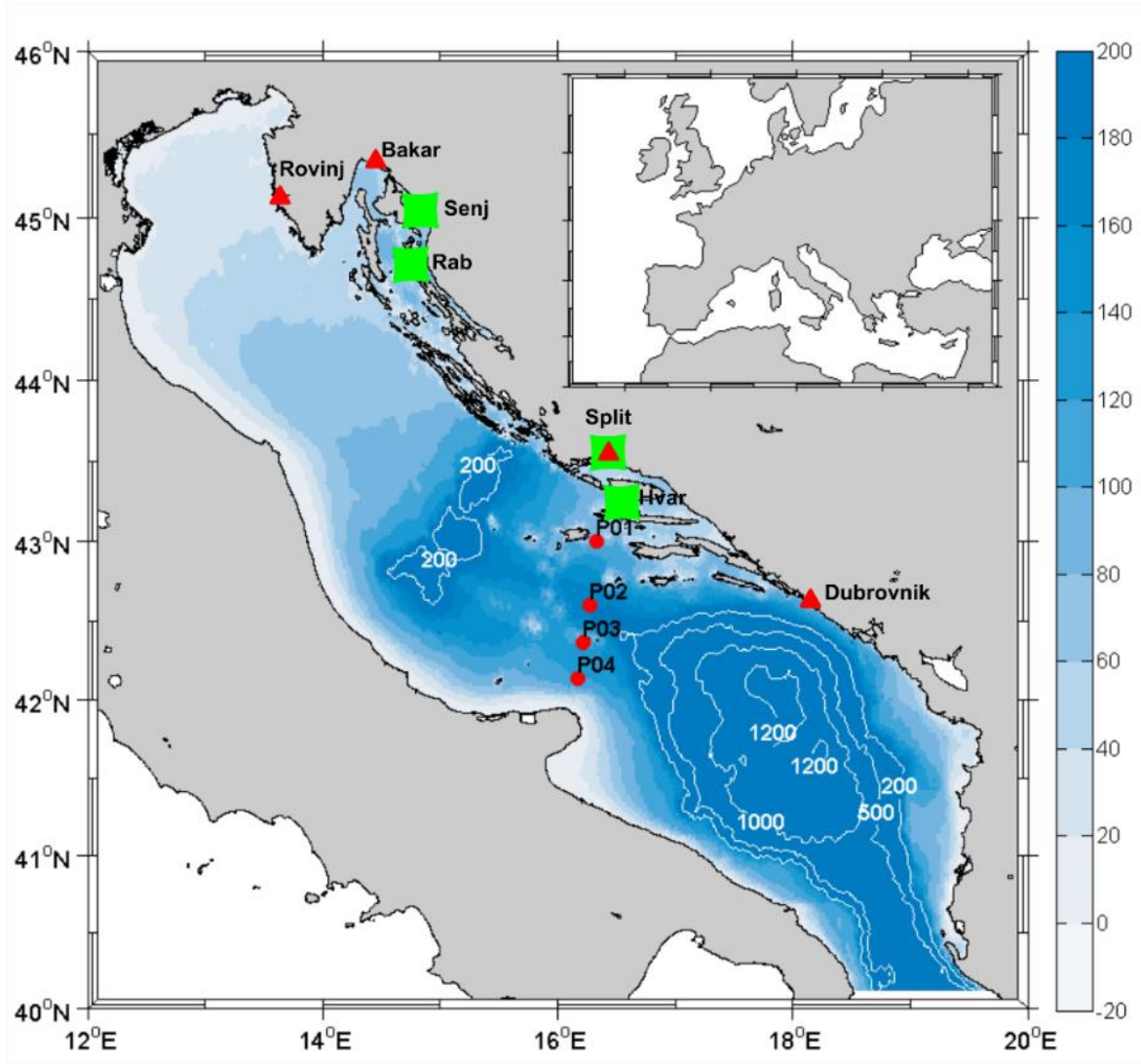


**Figure 5.1** Map of the Adriatic Sea with positions of SST Senj, Rab, Split and Hvar denoted by green.

## TREND ANALYSES

Linear trend analysis was performed for stations with long-term SST measurements, i.e., for stations Rab, Senj, Split, Hvar and Stončica for the common period 1964–2015. To detect differences over seasons, trends were calculated for each month separately using time series of monthly averages for that particular month during warming period 1979–2015. Additionally, a nonparametric locally weighted regression model (LOWESS) was fitted to the annual means (Cleveland 1979). LOWESS is a data analysis technique for producing a “smooth” set of values from a time series. Results of LOWESS analysis can vary with the size of the smoothing window. This size is given as the fraction (0–1) of the data that the window should cover. For example, a window size of 0.1 indicates that the smoothing window has a total width of 10% of the horizontal axis variable. We used the fraction 0.25, i.e., the smoothing window has a total width of 25% (e.g., 12.5 years for the 50-year time period).

## RESULTS

### *Trends, Variability and Extremes*

Seasonal decompositions of mean monthly SST values showed two distinctive periods at all investigated stations: (i) a cooling trend prior to 1979, and (ii) substantial warming thereafter (Figure 5.2). Taking only the period before 1979 into account, the linear trend was negative, varying from  $-0.28$  °C/decade for the station Rab to  $-0.56$  °C/decade for Split area (Table 4.1). The negative trend is more pronounced in the middle Adriatic area than in its northern part. The trend was reversed in the period 1979–2015, with positive values ranging from  $0.22$  to  $0.32$  °C/decade, ending in a total SST increase of about  $1.1$  °C during the whole period. The warming has particularly intensified since 2008, with trends as high as  $1.56$  °C/decade. The SST trends differed over seasons and months (Figure 5.3). The largest trends were found in spring and summer, i.e., in July in Senj and Rab, and in May in Split and Hvar. The highest monthly positive trends are:  $0.55$  °C/decade for Senj and  $0.40$  °C/decade for Rab in summer, and  $0.47$  °C/decade for Hvar and  $0.43$  °C/decade for Split in spring. These trends are higher than the increase in the other months, it is necessary to look for the cause. The spring and summer maximum of a multi-year trend can be associated with the minimum salt content in the surface layer. Namely, it is known that the seasonal surface salinity has two minimums both occurred in the warm part of the year: the first in the spring, and the second in the summer.

Obtained SST trends follow the findings for the atmospheric variables, where warming was also more pronounced during summer than winter (Branković et al. 2013). The lowest SST trends in the whole eastern Adriatic were in autumn (September–October), at the time of year when the thermocline is normally weakened and destroyed through vertical mixing driven by cyclonic activity (Buljan and Zore-Armanda 1976). In addition, air temperature trends along the Adriatic coastline were also found to be the lowest at that time of year (Branković et al. 2013).

**Table 4.1.** Sea surface temperature linear trends for stations along the eastern Adriatic coast and for the open sea station for the sub-periods A and B

Data source	Station	Period A	°C/decade	Decrease [°C]	Period B	°C/decade	Increase [°C]
MMS/MHS	Senj	1964–1978	– 0.295	– 0.443	1979–2015	+ 0.293	1.08
	Rab		– 0.276	– 0.497		+ 0.226	0.84
	Split		– 0.560	– 1.120		+ 0.315	1.17
	Hvar		– 0.417	– 0.626		+ 0.296	1.10
IOF	Stončica		– 0.427	– 0.811		+ 0.230	0.85
	All stations		– 0.395	– 0.699		+ 0.272	1.01

Trend analysis of sea surface temperature in the eastern Adriatic Sea, from the coastal area to the open sea, show that since 1979 the surface temperature has increased, more precisely it is oscillating around higher values. In the period from 1979 to 2015, the increase was 1.03 °C, which is in line with the warming trend of the sea surface in the other Mediterranean areas. The positive trend has been more pronounced in recent decades. Between 2008 and 2015 the surface layer temperature of the sea has increased by 1.25 °C. This trend of strong warming continues, which does not preclude strong cooling episodes occurrence at the future climate. The extremes should be particularly monitored, as their frequency is expected to increase with projected climate change (Jacob et al. 2014).

Sea temperature trends along the eastern coast of the Adriatic are neither spatially nor seasonally homogeneous. Where the sea is shallower and under the influence of fresh water (precipitation and / or freshwater from the land) it responds faster to changes.

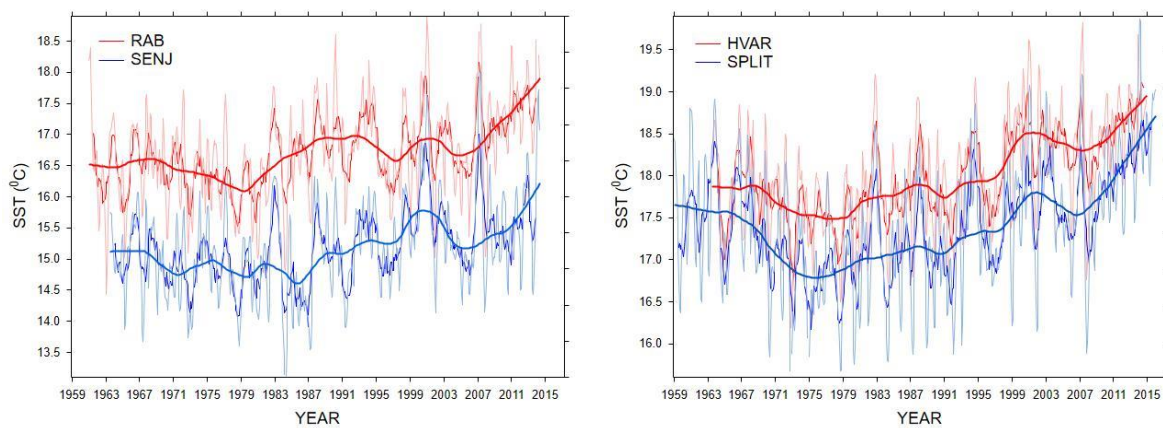


**Figure 5.2** Seasonal decompositions of mean monthly sea surface temperature for the eastern Adriatic stations Rab, Senj Split and Hvar obtained from moving averages procedure. Non-linear trends are presented as LOWESS spline (bold lines).

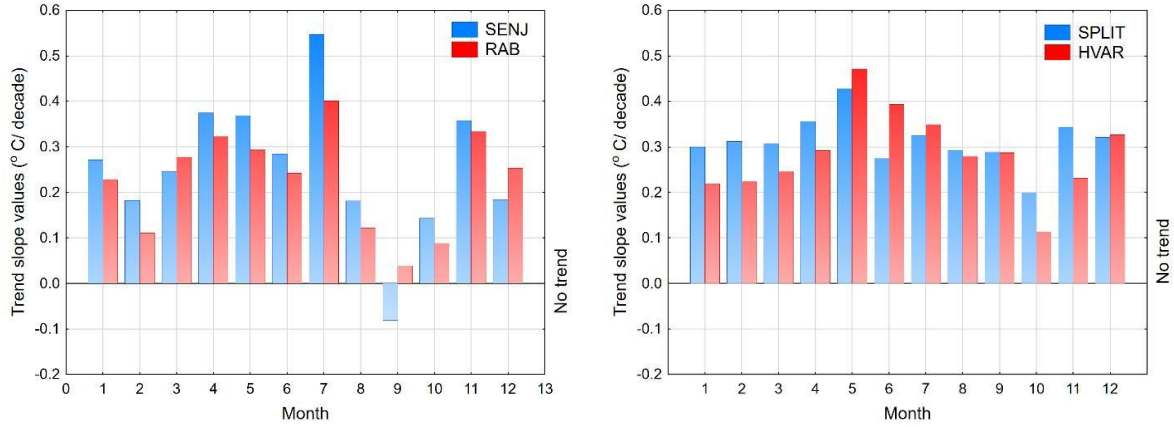


**Figure 5.3** Monthly linear SST trends for the warming period 1979–2015 at selected stations.

Surface temperatures of the sea in May, the month with the highest positive multi-year trend, are quite variable. The average May value for Split is 17.6 °C, and for Hvar 17.5 °C. The minimum value was recorded in 1992 and for Split it was 15.0 °C and for Hvar 15.6 °C. The maximum was in 2000 and with value of 20.6°C, and for Hvar of 20.5°C (Figure 5.4).

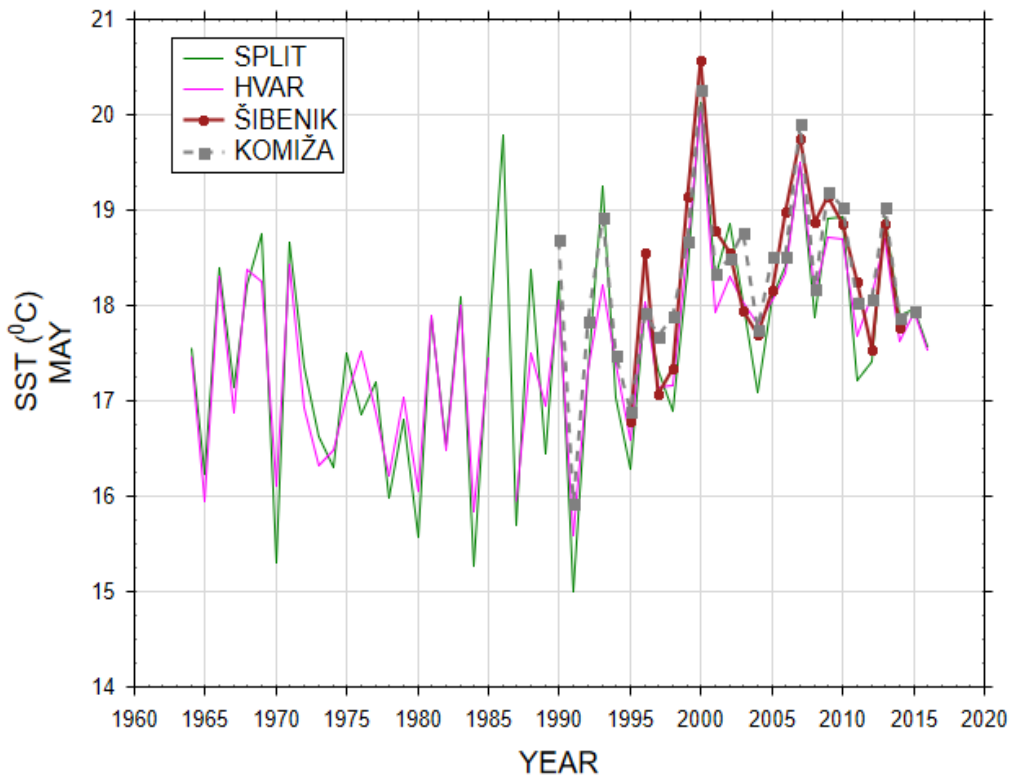


**Figure 5.4** Long-term SST changes for May in the middle Adriatic Sea at selected stations.

We further focused on winter variability and trends (Figure 5.5), in particular for February when minimum temperatures were reached (Supić et al. 2004) and dense water formation occurs on the northern Adriatic shelf (Zore-Armanda 1969). These trends are estimated at rates between 0.09 °C/decade (Rab) and 0.16 °C/decade (Hvar), indicating that warming also exists in the cold part of the year. Yet, strong variability was observed, with extremely (above two standard deviations) cold winters occurring in 1963, 1981 and 2012, and mild winters observed in 2001, 2007 and 2014. These anomalies are, as expected, tied to the prevailing synoptic situations over Europe illustrated with February air temperature anomalies (see Grbec, et al. 2018). For example, weather conditions during the winter of 2007 were unusual, with air temperatures over the Adriatic two standard deviations over the mean values. Such a situation was the result of a weakening of the Siberian anticyclone, which in normal winters occasionally brings colder air masses and bora wind outbursts (Grisogono and Belušić 2009) from continental Europe. At the same time, warm air masses were advected from the southwest (Luterbacher et al. 2007), particularly over the northern Adriatic. Because of a warmer atmosphere in the northern Adriatic, surface layer cooling was reduced and North Adriatic Dense Water (NAdDW) formation was missing (Oddo and Guarneri 2011). Mean monthly sea surface temperatures during February 2007 were considerably higher than long-term means, with temperature anomalies ranging from 0.67 °C in Komiža to 1.23 °C in Senj.

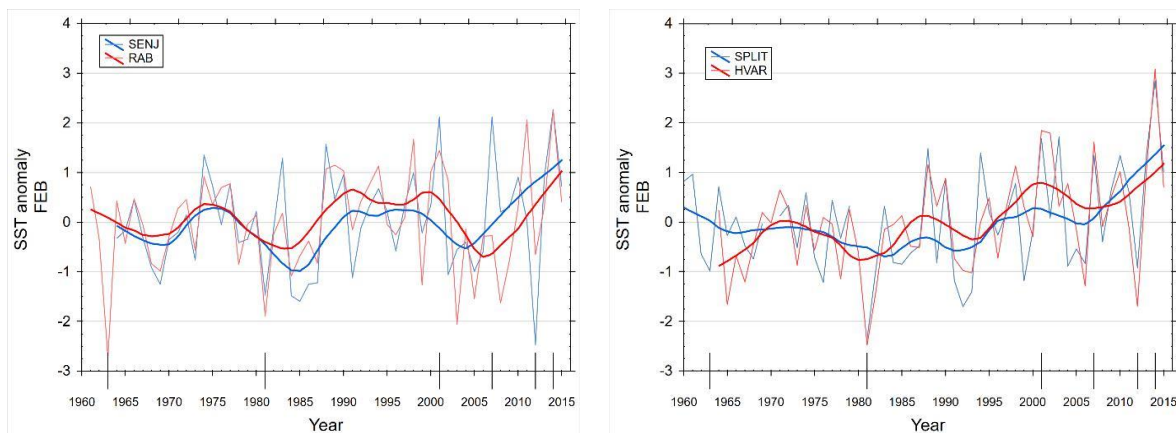


**Figure 5.5** Time series of mean sea surface temperature anomalies in February, for stations Senj, Rab, Split and Hvar. Crossed tick marks indicate extremely cold and mild February (values below/above two standard deviations). Trends were presented with locally weighted scatterplot smoothing (LOWESS) method.

A completely different synoptic situation prevailed during the winter of 2012 (Mihanović et al. 2013; Gačić et al. 2014). Combined cyclonic activity and atmospheric blocking over both the Mediterranean and Atlantic were responsible for a pronounced and long-lasting advection of cold air masses over the Adriatic and an extreme bora wind spanning over late January and February. Adriatic February air temperatures were about 2°C lower than average. Consequently, in situ SST at Senj was 3°C lower than average, while the temperature negative anomalies were lower at stations placed further offshore. Aside from differences in the synoptic conditions, a common characteristic of all anomalous events is the existence

of atmospheric blocking situations and intensified omega planetary circulation (not shown), which is a result of energy transfer between subtropical and polar regions. Depending on the position and outreach of the blockage, the Adriatic experienced either prolonged advection of warm air from the subtropical belt, or cold air from northern Europe or Siberia.

In addition, sea surface temperature observations are presented for the Otranto (period 1998-2018; Fig. 5.6) and Bari (period 1998-2016; Fig. 5.7). Linear trend after removing the seasonal cycle shows warming with 0.4 °C/10 years in Otranto and 0.8 °C/10 years in Bari.

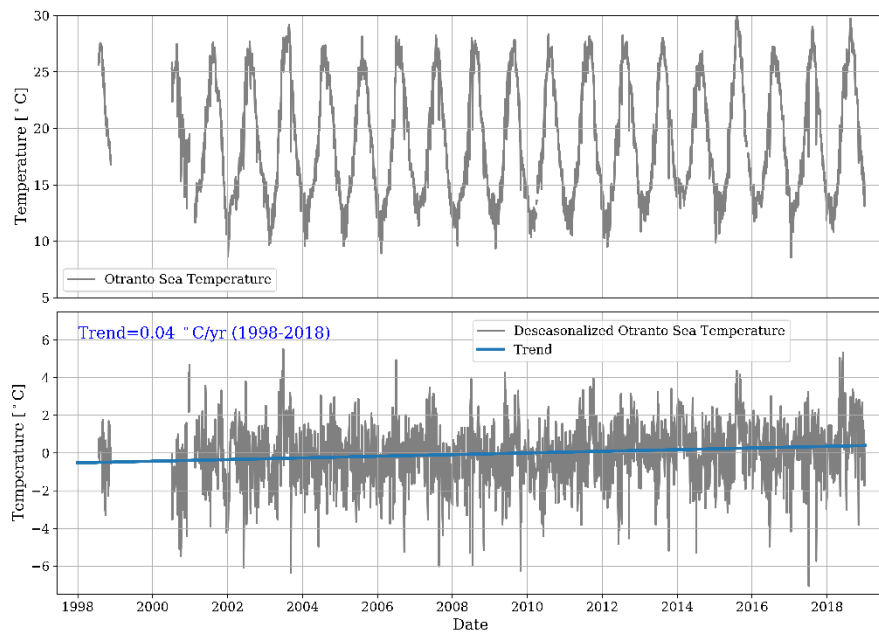


**Figure 5.6** Sea surface temperature observed in Otranto (1<sup>st</sup> row). Seasonal cycle removed from the original time-series and linear trend estimated for Otranto observations (2<sup>nd</sup> row).

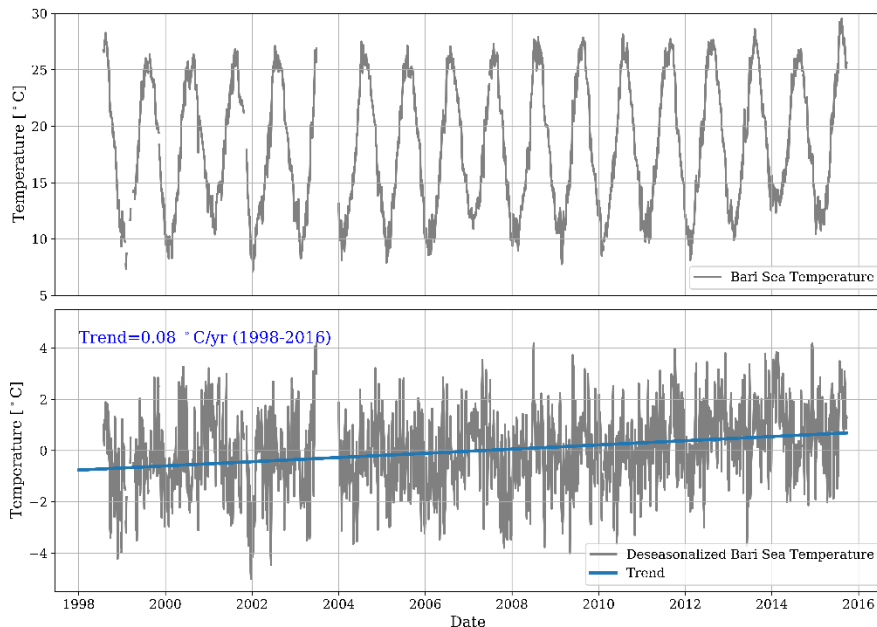


**Figure 5.7** Sea surface temperature observed in Bari (1<sup>st</sup> row). Seasonal cycle removed from the original time-series and linear trend estimated for Bari observations (2<sup>nd</sup> row).

## CONCLUSION AND DISCUSSION

Monthly and yearly averages used to document SST trends and variability, revealed the dominance of temporal changes with respect to the effects of spatial differences in SST anomalies, indicating the prevalence of hemispheric processes over local dynamics, such as bora wind spatial inhomogeneity. SST extremes were connected with blocking atmospheric patterns. A substantial warming between 1979 and 2015, in total exceeding 1 °C, was preceded by a period with a negative SST trend, implying strong multidecadal variability in the Adriatic. The strongest connection was found between yearly SST and the East Atlantic (EA) pattern, while North Atlantic Oscillation (NAO) and East Atlantic/West Russia (EAWR) patterns were found to also affect February SST values. Quantification of the Adriatic SST and their connection to hemispheric indices allow for more precise projections of future SST, considered to be rather important for Adriatic thermohaline circulation, biogeochemistry and fisheries, and sensitive to ongoing climate change.

## 6 Sea level trends in the Adriatic

Sea level trends in the Adriatic Sea have been computed from monthly data collected at four long operating tide gauges: Rovinj (1955-2014), Bakar (1929-2013), Split (1954-2014) and Dubrovnik (1956-2014). The data has been quality checked and retrieved from Permanent Service for Mean Sea Level ([www.psmsl.org](http://www.psmsl.org)), which is collecting sea level data from tide gauge stations all over the world. All but Bakar tide gauges are operated by Hydrographic Institute of the Republic of Croatia, while Bakar tide gauge is operated by University of Zagreb, Faculty of Science, Department of Geophysics. All tide gauge are float-type tide gauges in a stilling well.

Although the Bakar tide gauge is operating a bit longer than the other three tide gauge, there are several important conclusions which might be derived from the presented graphs (Figs. 6.1 to 6.4). First, the trend is apparently positive, although large interannual and decadal variability can be detected in the series. This variability may also affect the trend estimates, which are much higher when being computed over the period 1990-2014. A part of this trend is coming from period of low sea levels at the beginning of 1990s. However, the trend over the whole investigated interval is persistent and increasing from the north Adriatic to the south Adriatic - the trend at Dubrovnik is almost two times larger than at Rovinj. This has been also reflected in the 1990-2014 trend estimates. It is a question to research why there is such a difference, yet assuming the same amount of heating all over the Adriatic, it might be related to the water mass budget that is largely driven by rivers in the northern Adriatic.

In addition, sea level observations are presented for the Otranto (Fig. 6.5) and Bari (Fig. 6.6). Linear trend for the Otranto data shows sea level rising 3.74 mm/year in the period 1999-2018 (some earlier data may have observational systematic inconsistencies). Linear trend for the Bari data shows sea level rising 8.23 mm/year in the period 1999-2015 (some earlier data may have observational systematic inconsistencies similar to Otranto).

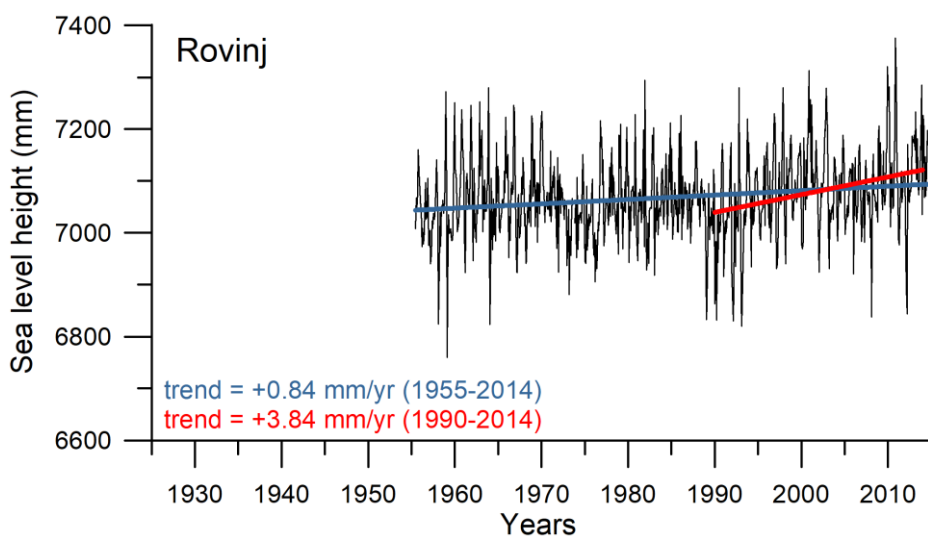


**Fig. 6.1** Time series of the sea level height (mm) for the location Rovinj. Linear trends for the periods 1955-2014 and 1990-2014 included.

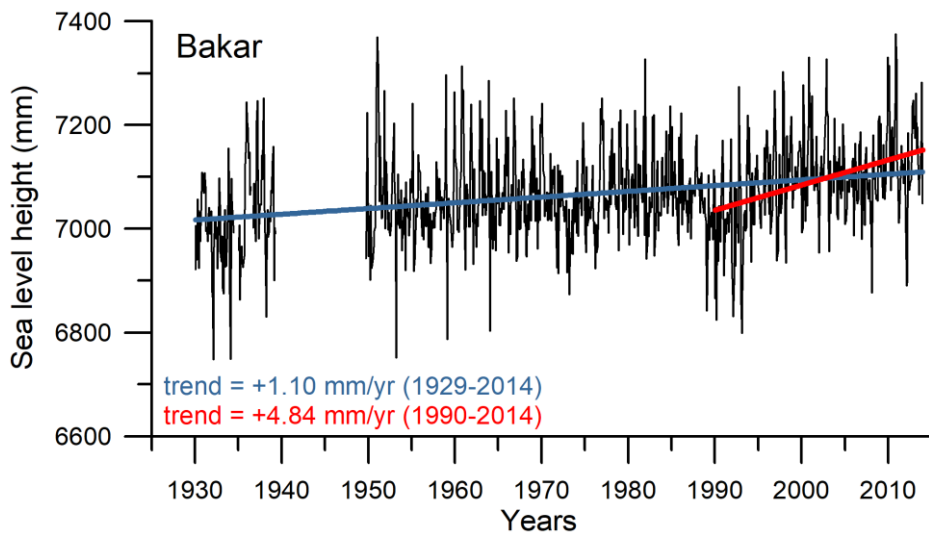


**Fig. 6.2** Time series of the sea level height (mm) for the location Bakar. Linear trends for the periods 1929-2014 and 1990-2014 included.

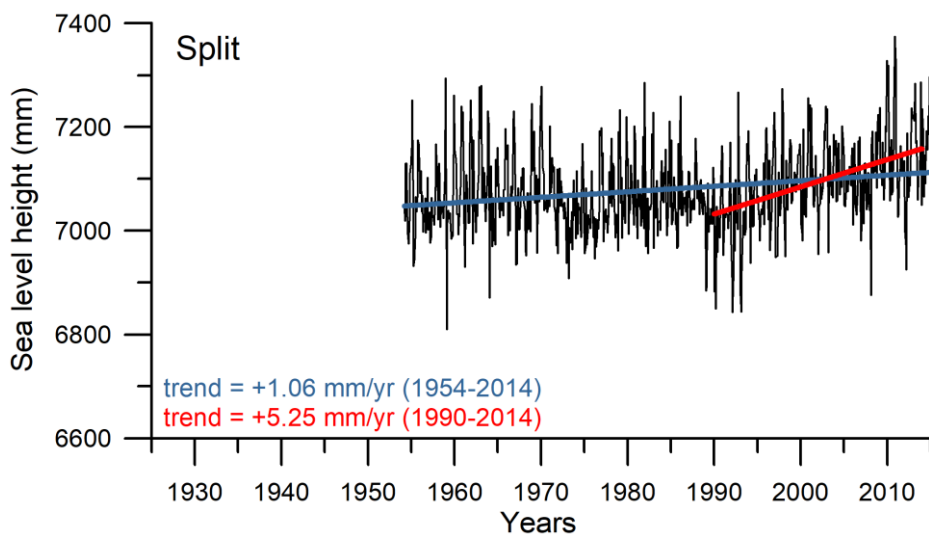


**Fig. 6.3** Time series of the sea level height (mm) for the location Split. Linear trends for the periods 1954-2014 and 1990-2014 included.

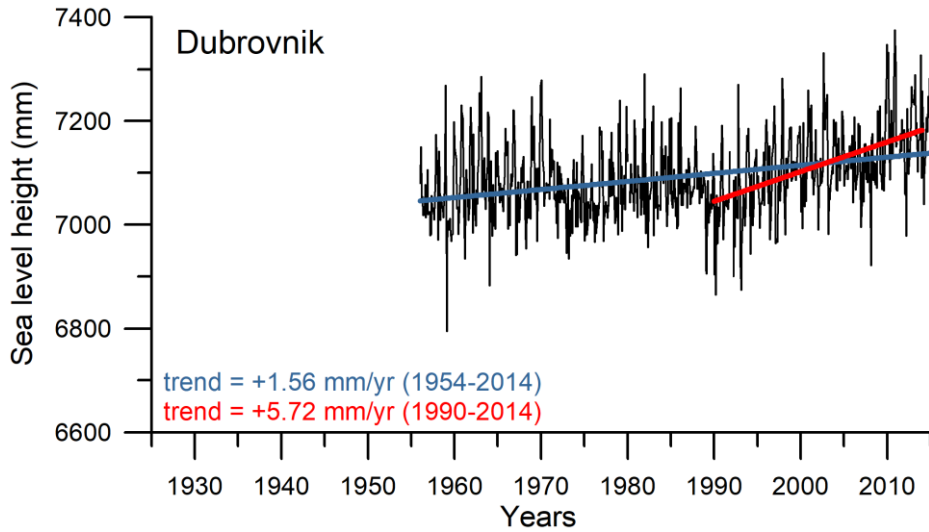


**Fig. 6.4** Time series of the sea level height (mm) for the location Dubrovnik. Linear trends for the periods 1954-2014 and 1990-2014 included.

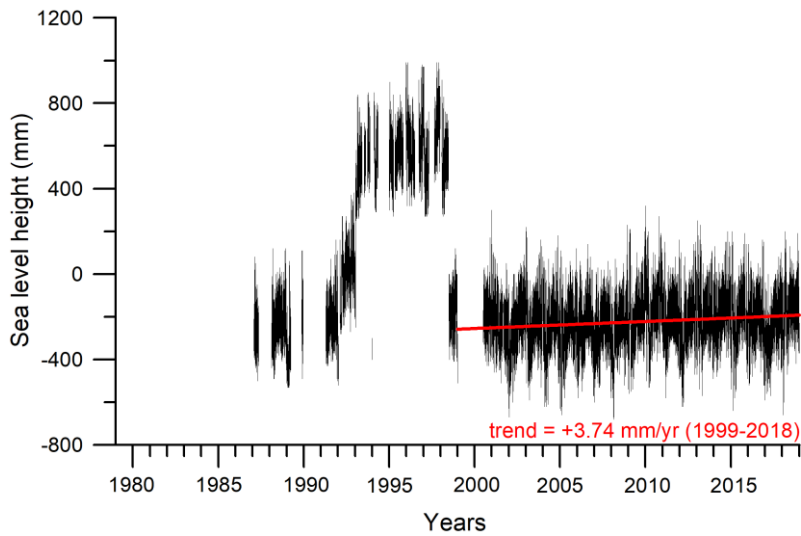


**Fig. 6.5** Time series of the sea level height (mm) for the location Otranto. Linear trend for the period 1999-2018.

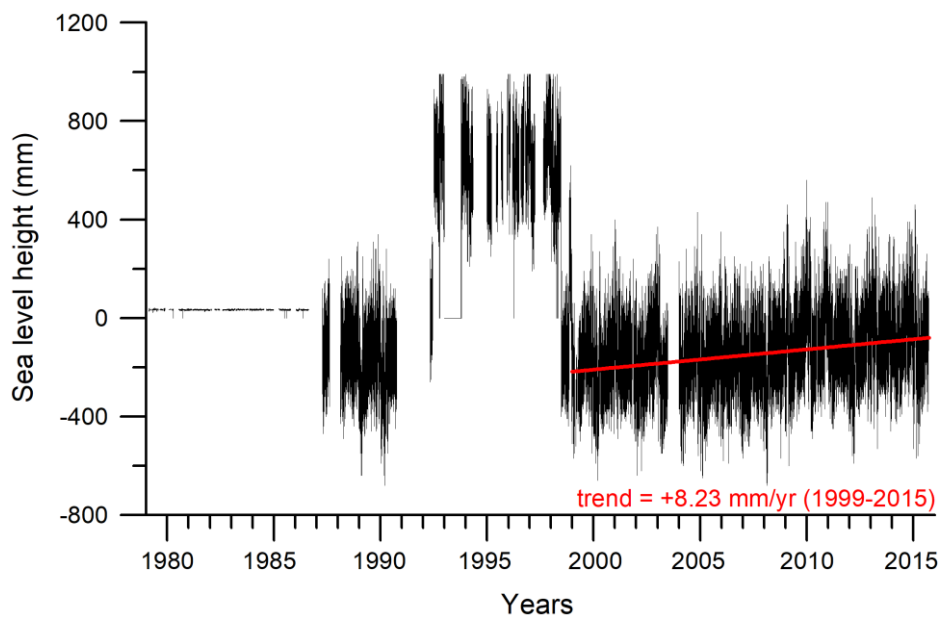


**Fig. 6.6** Time series of the sea level height (mm) for the location Bari. Linear trend for the period 1999-2015.

## 7 Sea temperature and salinity trends in the Adriatic transect

This subsection summarizes observations for the location P01 at the Adriatic transect (cf. Fig. 5.1). Sea temperature linear trend for period 1963-2016 has slope  $0.48\text{ }^{\circ}\text{C}/100\text{ years}$ , and for period 1993-2016 has slope  $6.55\text{ }^{\circ}\text{C}/100\text{ years}$  (Fig. 7.1, upper panel). Salinity linear trend for period 1963-2016 has slope  $0.22\text{ PSU}/100\text{ years}$ , and for period 1993-2016 has slope  $1.37\text{ PSU}/100\text{ years}$  (Fig. 7.1, lower panel).

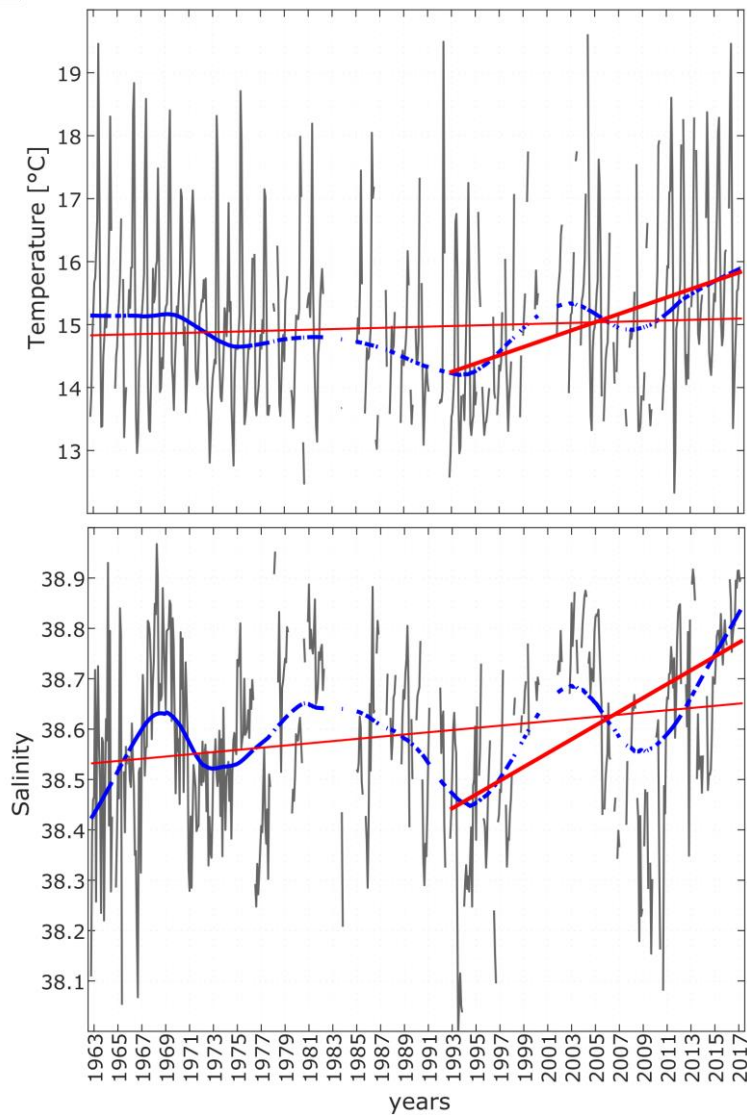


**Figure 7.1** Time evolution of sea temperature (upper panel) and salinity (lower panel) for station P01 averaged for depths between 30 m and 100 m. Original data are shown in gray, LOWEST low pass filtered in blue and trend in red color.

## Acknowledgements

We acknowledge the E-OBS dataset from the EU-FP6 project UERRA (<http://www.uerra.eu>) and the Copernicus Climate Change Service, and the data providers in the ECA&D project (<https://www.ecad.eu>).

We also acknowledge Italian and Croatian providers of the local climate data for the purpose of this report.

In particular, concerning Apulia Region, we acknowledge the Civil Protection (Centro Funzionale Decentrato – Sezione Protezione Civile – Regione Puglia) for temperature and precipitation data and the Mareographic National Network (Rete Mareografica Nazionale – ISPRA) for sea data.

CIT and wind analysis presented in this report based on the ERA5, i.e. modified Copernicus Climate Change Service information (2019). Neither the European Commission nor ECMWF is responsible for any use that may be made of the Copernicus Information or Data it contains.

## References

- Bafaluy D, Amengual A, Romero R, Homar V (2014) Present and future resources for various types of tourism in the Bay of Palma, Spain. *Reg Environ Change*, 14: 1995–2006.
- Branković Č, Güttler I, Gajić-Čapka M (2013) Evaluating climate change at the Croatian Adriatic from observations and regional climate models' simulations. *Climate Dynamics*, 41: 2353–2373.
- Buljan M, Zore-Armanda M (1976) Oceanographic properties of the Adriatic Sea. *Oceanography and Marine Biology Annual Review*, 14: 11–98.
- Cleveland WS (1979) Robust Locally Weighted Regression and Smoothing Scatterplots. *Journal of the American Statistical Association*. doi:10.2307/2286407.
- Copernicus Climate Change Service (C3S) (2017): ERA5: Fifth generation of ECMWF atmospheric reanalyses of the global climate . Copernicus Climate Change Service Climate Data Store (CDS), *September 2019*. <https://cds.climate.copernicus.eu/cdsapp#!/home>
- Cornes R, van der Schrier G, van den Besselaar EJM, Jones PD (2018) An Ensemble Version of the E-OBS Temperature and Precipitation Datasets. *J. Geophys. Res. Atmos.*, 123, doi:10.1029/2017JD028200
- Cox RA, Drews M, Rode C & Nielsen SB (2015) Simple future weather files for estimating heating and cooling demand. *Build Environ*, 83: 104–114.
- De Freitas CR, Scott D, McBoyle G (2008) A second generation climate index for tourism (CIT): specification and verification. *Inr J Biometeorol* 52: 399–407.
- Gačić M, Civitarese G, Kovačević V, Ursella L, Bensi M, Menna M, Cardin V, Poulain P-M, Cosoli S, Notarstefano G, Pizzi C (2014) Extreme winter 2012 in the Adriatic: an example of climatic effect on the BiOS rhythm. *Ocean Science*, doi:10.5194/os-10-513-2014.
- Grbec, B (1997) Influence of climatic changes on oceanographic properties of the Adriatic Sea. *Acta Adriatica* 38(2): 3–29.
- Grbec B, Morović M (1997) Seasonal thermohaline fluctuations in the middle Adriatic Sea. *Il Nuovo Cimento C*, 20: 561–576.
- Grbec B, Morović M, Beg Paklar G, Kušpilić G, Matijević S, Matić F, Gladan Ž N (2009) The relationship between the atmospheric variability and productivity in the Adriatic Sea area. *Journal of the Marine Biological Association of the UK*, 89: 1549–1558.
- Grbec B, Matić F, Beg Paklar G, et al. (2018) Long-Term Trends, Variability and Extremes of In Situ Sea Surface Temperature Measured Along the Eastern Adriatic Coast and its Relationship to Hemispheric Processes. *Pure Appl. Geophys.*, Springer International Publishing AG, part of Springer Nature <https://doi.org/10.1007/s00024-018-1793-1>.

Grisogono B, Belušić D (2009) A review of recent advances in understanding the meso- and microscale properties of the severe Bora wind. *Tellus A*, 61: 1–16.

Hopes P (1999) The physiological equivalent temperature - a universal index for the biometeorological assessment of the thermal environment. *Int J Biometeorol* 43: 71–75.

Jacob J, Petersen J, Eggert B, Alias A, Christensen OB, Bouwer LM, Braun A, Colette A, Déqué M, Georgievski G, Georgopoulou E, Gobiet A, Menut L, Nikulin G, Haensler A, Hempelmann N, Jones C, Keuler K, Kovats S, Kröner N, Kotlarski S, Kriegsman A, Martin E, van Meijgaard E, Moseley C, Pfeifer S, Preuschmann S, Radermacher C, Radtke K, Rechid D, Rounsevell M, Samuelsson P, Somot S, Soussana J-F, Teichmann C, Valentini R, Vautard R, Weber B, Yiou P (2014) EURO-CORDEX: new high-resolution climate change projections for European impact research. *Regional Environmental Change*, 14: 563–578.

Luterbacher J, Liniger MA, Menzel A, Estrella N, Della-Marta PM, Pfister C, Rutishauser T, Xoplaki E (2007) Exceptional European warmth of autumn 2006 and winter 2007: Historical context, the underlying dynamics, and its phenological impacts, *Geophysical Research Letters*, doi:10.1029/2007GL029951.

Lorenz JR (1863) *Physikalische Verhältnisse und Verteilung der Organismen im Quarnerischen Golfe*. Hofund Staatsdruckerei, Wien.

Matić F, Grbec B, Morović M (2011) Indications of climate regime shifts in the middle Adriatic Sea. *Acta Adriatica*, 52: 235–246.

Matzarakis A, Mayer H, Iziomon MG (1999) Application of a universal thermal index: physiological equivalent temperature. *Int J Biometeorol* 43: 76–84.

Mihanović H, Vilibić I, Carniel S, Tudor M, Russo A, Bergamasco A, Bubić N, Ljubešić Z, Viličić D, Boldrin A, Malačić V, Celio M, Comici C, Raicich F (2013) Exceptional dense water formation on the Adriatic shelf in the winter of 2012. *Ocean Science*, 9: 561–572.

Oddo P, Guarnieri A (2011) A study of the hydrographic conditions in the Adriatic Sea from numerical modelling and direct observations (2000–2008). *Ocean Science*, 7: 549–567.

Supić N, Orlić M (1992) Annual cycle of sea surface temperature along the east Adriatic coast. *Geofizika*, 9: 79–97.

Supić N, Grbec B, Vilibić I, Ivančić I (2004) Long-term changes in hydrographic conditions in northern Adriatic and its relationship to hydrological and atmospheric processes. *Annales Geophysicae* 22: 733–745.

Vilibić I, Šepić J, Proust N (2013) Weakening of thermohaline circulation in the Adriatic Sea. *Climate Research*, 55: 217–225.

Zore-Armanda M (1969) Temperature relations in the Adriatic Sea. *Acta Adriatica*, 13(5): 1–51.

Zore-Armanda M, Bone M, Dadić V, Morović M, Ratković D, Stojanoski L, Vukadin I (1991) Hydrographic properties of the Adriatic Sea in the period from 1971 through 1983. *Acta Adriatica*, 32/1: 1–552.

## Appendix: Station observations of the meteorological parameters

**Table A1** Basic meta-data of the analysed meteorological observations.

Station name	Long (deg)	Lat (deg)	Area	Provider or means of providing
<i>Cres</i>	14.42	44.95	HR	DHMZ
<i>Šibenik</i>	15.92	43.73	HR	DHMZ
<i>Dubrovnik</i>	18.08	42.65	HR	DHMZ
<i>Pesaro</i>	12.90	43.90	IT (Marche)	Marche Regional Monitoring and Forecasting Center for Civil Protection
<i>Ancona</i>	13.05	43.60	IT (Marche)	Marche Regional Monitoring and Forecasting Center for Civil Protection
<i>Giulianova</i>	13.95	42.73	IT (Abruzzo)	Idrographic office of Abruzzo Region
<i>Pescara</i>	14.23	42.43	IT (Abruzzo)	Idrographic office of Abruzzo Region
<i>Ortona</i>	14.40	42.03	IT (Abruzzo)	Idrographic office of Abruzzo Region
<i>Torino di Sangro</i>	14.53	42.23	IT (Abruzzo)	Idrographic office of Abruzzo Region
<i>Brindisi</i>	17.93	40.63	IT (Puglia)	<a href="https://www.ecad.eu//dailydata/predefine_dseries.php">https://www.ecad.eu//dailydata/predefine_dseries.php</a> / Puglia
<i>Badia Polesine/Masi</i>	11.50	45.09	IT (Veneto)	ARPAV
<i>Rovigo/Concadirame</i>	11.77	45.08	IT (Veneto)	ARPAV
<i>Portogruaro/Lison Portogruaro</i>	12.84	45.78	IT (Veneto)	ARPAV
<i>Legnaro/Legnaro</i>	11.95	45.35	IT (Veneto)	ARPAV
<i>Venezia Cavanis Institute</i>	12.33	45.43	IT (Veneto)	ARPAV
<i>S. Nicolo' di Lido / Cavallino Treporti</i>	12.38	45.43	IT (Veneto)	ARPAV
<i>Bonifica Vittoria / Fossalon di Grado</i>	13.13	45.73	IT (FVG)	via ARPAV
<i>Pordenone / Pordenone loc. Torre</i>	12.67	45.97	IT (FVG)	via ARPAV
<i>Udine</i>	13.25	46.07	IT (FVG)	via ARPAV
<i>Classe</i>	12.24	44.37	IT (Emilia-Romagna)	via ARPAV
<i>Bologna</i>	11.35	44.50	IT (Emilia-Romagna)	via ARPAV

<i>Cesena</i>	12.22	44.14	IT (Emilia-Romagna)	via ARPAV
<i>Cesenatico</i>	12.40	44.21	IT (Emilia-Romagna)	via ARPAV
<i>Rimini</i>	12.58	44.06	IT (Emilia-Romagna)	via ARPAV
Lignano Sabbiadoro	13.11	45.67	IT (FVG)	
Montemarciano	13.31	43.64	IT (Marche)	
<i>Brindisi</i>	17.93	40.64	IT (Puglia)	Apulian Civil Protection (Centro Funzionale Decentrato – Sezione Protezione Civile – Regione Puglia)
<i>Latiano</i>	17.71	40.55	IT (Puglia)	Apulian Civil Protection (Centro Funzionale Decentrato – Sezione Protezione Civile – Regione Puglia)
<i>Otranto</i>	18.49	40.14	IT (Puglia)	Apulian Civil Protection (Centro Funzionale Decentrato – Sezione Protezione Civile – Regione Puglia)
<i>Polignano</i>	17.22	40.99	IT (Puglia)	Apulian Civil Protection (Centro Funzionale Decentrato – Sezione Protezione Civile – Regione Puglia)
<i>S. P. Vernotico</i>	18.00	40.48	IT (Puglia)	Apulian Civil Protection (Centro Funzionale Decentrato – Sezione Protezione Civile – Regione Puglia)
<i>S. V. dei Normanni</i>	17.71	40.66	IT (Puglia)	Apulian Civil Protection (Centro Funzionale Decentrato – Sezione Protezione Civile – Regione Puglia)